TECHNISCHE UNIVERSITÄT WIEN
Vienna | Austria

D I P L O M A R B E I T

Radiation Qualities for Calibration of Dosimeters used in Mammography

Dosimetry and Medical Radiation Physics Section
IAEA

Zentrum für Medizinische Physik und Biomedizinische Technik
Medizinische Universität Wien

Atominstitut
Technische Universität Wien

Ao.Univ.Prof. Dipl.-Ing. Dr.techn. Peter Homolka
Adj. Prof. Paula Toroi, MSc, PhD

Elisabeth Salomon, BSc
1060 Wien, Garbergasse 7/9

24.01.2018

_____

Contents

1

Abstract

For comprehensive quality control measurements in diagnostic radiography the number of semiconductor-based dosimeters is increasing. These compact dosimeters are, compared with ionization chambers, easy to handle and they provide several quantities with one exposure. Their inherent energy dependence of their response is more pronounced than for ionization chambers. Therefore, multiple compensation methods based on the radiation quality are developed by the manufacturers. To ensure that dosimeters are working correctly they should be calibrated regularly.

The conditions in the calibration laboratory may vary significantly from the clinical ones. The range of clinically used radiation qualities is large and depends on the type of X-ray machine. However, for calibration only a limited set of radiation qualities are available at the calibration laboratories. The international standard IEC 61267 [1] specifies the conditions for use in the determination of characteristics of diagnostic dosimeters. It includes mammographic X-ray beam qualities only based on Mo-Mo anode-filter combinations.

Energy dependence of the response of eight semiconductor dosimeters and one ionization chamber were determined for clinically used radiation qualities with five different anode-filter combinations in tube voltage range from 25 kV to 35 kV. The maximum variations for six dosimeters were within the ±5% required by the IEC 61674 [2] standard. If a dosimeter is calibrated only with the standard radiation quality Mo-Mo 28, the correction for the use with other radiation qualities can be up to 12%. The HVL and high voltage measurement functions were also tested, if available. For each beam quality the maximum variation was within 11% and 10%, respectively.

Normally, the internal compensation of the energy dependence of response requires preselection of the radiation quality in the dosimetry software. If the radiation quality differs from the selected one, the maximum variation remains in the 5% range only in case of three dosimeters. To simulate the clinical radiation condition with compression paddle in the beam radiation qualities with additional filtration of PMMA were established. Even if the nominal radiation quality (anode-filter combination and tube voltage) is the same in calibration and clinical measurement, the additional filtration changes the spectra so that the response can increase up to 16%.

This extended test demonstrates the radiation quality dependence of the response of semiconductor dosimeters. As well as provides some details about the built-in energy compensation applied. Based on this study errors and uncertainties related to different measurement and calibration scenarios can be estimated.

2 Introduction

2.1 Mammography

Breast cancer is the most common cancer among women worldwide and is a leading cause of cancer mortality in women. Early detection, in order to improve outcome and survival, remains the cornerstone of breast cancer control. So far, the only breast cancer screening method that has proved to be effective is mammography screening. There is evidence that organized population-based mammography screening programs can reduce breast cancer mortality by around 20% [3].

Mammography is an X-ray imaging of the breast. The radiological signs of breast cancer include masses that show typical slightly higher X-rays attenuation than surrounding normal tissue, small microcalcifications, asymmetry between the two breasts and architectural distortion of tissue patterns. To detect breast cancer accurately and at the earliest possible stage, the image must have excellent contrast, spatial resolution and adequate latitude to reveal any pathology characteristic of cancer. In addition, the X-ray dose must be as low as reasonably achievable to minimize harmful effects of ionization radiation. The rate of radiation-induced breast cancer due to mammography screening is estimated to 1.6‰ for biennial screening in women aged 50-74 years [4]. A scheme and picture of a mammography machine is shown in Figure 2.1.

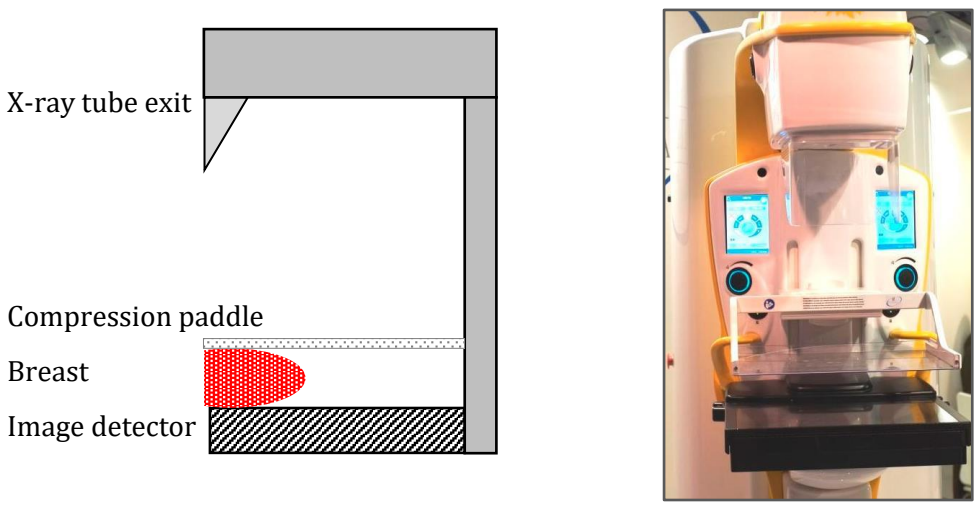

Figure 2.1: Scheme and picture of a mammography machine.

2.2 Dose quantities

The incident air kerma (2.1) is the sum of the initial kinetic energies *dE* of all charged particles liberated by uncharged particles in a mass *dm*. The air kerma rate is the air kerma per unit time (2.2).

$$K_{air}\,[Gy] = \frac{dE\,[J]}{dm\,[kg]} \tag{2.1}$$

$$\dot{K}_{air}[Gy/s] = \frac{dK_{air}\,[Gy]}{dt\,[s]} \tag{2.2}$$

The primary quantity of interest is the mean glandular dose MGD (other term: average glandular dose AGD). It is a patient and risk related quantity and describes the mean dose to glandular tissue within the breast, described by a standard breast model. It is estimated from the incident air kerma K_{air} (without backscatter from the breast) using Monte Carlo calculated conversation factors g, s and c (see equation (2.3)). The g-factor was introduced in 1990 by Dance and converts the incident air kerma for a breast of 50% glandularity to mean glandular dose. At that time, the g-factor was tabulated against breast thickness and half-value layer. In 2000 allowance was made for the dependence of the dose for a given half-value layer and breast thickness on the anode-filter combinations. Therefore, the factors s and c were introduced which accounted for the use of different X-ray spectra (Mo-Mo, Mo-Rh, Rh-Rh and W-Rh anode-filter combinations) and for breasts of different glandularities (0.1%, 25%, 50%, 75% and 100%), respectively. In 2009 further s-factors for W-Ag and W-Al were published [5]–[7].

$$MGD = K_{air} * g * s * c \tag{2.3}$$

2.3
Dosimeters used in mammography

Special radiation conditions in mammography, as lower tube voltages, photon energies and a variety of anode filter combinations set high standards on dosimeters used for this purpose. The International Standard 61674 [2] defines requirements for a satisfactory level of performance and standardizes the methods for the determination of compliance with this level of performance. Under reference conditions limits of variation of ±5% for the energy dependence of response are required. Variation is the relative difference between the values of a performance characteristic - which is the quantity used to define the performance of an instrument - when one influence quantity changes and one keeps the same. Any quantity which may affect the performance of an instrument is an influence quantity. The limits of variation are the maximum permitted variation of a performance characteristic.

According to this International Standard, diagnostic dosimeters are defined as "*equipment which uses **ionization chambers** and/or **semiconductor detectors** for the measurement of air kerma, air kerma length product and/or air kerma rate in the beam of an X-ray equipment used for diagnostic medical radiological examinations*."
A diagnostic dosimeter contains the following components:

Detector assembly: Radiation detector and all other parts to which the radiation detector is permanently attached. The radiation detector is the element which transduces air kerma, air kerma length product or air kerma rate into a measurable electrical signal as an ionization chamber or semiconductor detector.

Measuring assembly: measure charge (or current) from the radiation detector and convert it into a form suitable for displaying the values of dose or kerma or their corresponding rates.

2.3.1
Ionization Chambers

In principal, an ionization chamber is a radiation detector which derives an electronic output signal that originates with the ion pairs formed by the passage of radiation within the detector volume. The drift of the positive and negative charges in the presence of the electric field within the ionization chamber results in the ionization current. The practical quantity of interest is the total number of ion pairs created along the track of the radiation since it is proportional to the deposited energy.

For the energy range of the radiation used in mammography vended, plan parallel ionization chambers are used. Vended ionization chambers are constructed in a way to allow the air inside the measuring volume to communicate freely with the atmosphere. Therefore, corrections to the response for changes in air density need to be made. Plane parallel ionization chambers use two parallel, flat electrodes to create the electrical field within the volume of the chamber. To reduce the leakage current, a third electrode (guard) is surrounding the collecting electrode, to allow any leakage to flow to ground. A scheme of a plane parallel ionization

chamber is shown in Figure 2.2.

The range in air of secondary electrons created by mammographic X-rays is less than 1 cm. In the ideal case one would need to follow each secondary electron over its entire range to measure all the ionization created along its track. That means that all ionization charge created outside the active volume from secondary electrons that were formed within the active volume is exactly balanced by charge created within the active volume from secondary electron formed in the surrounding air. This secondary electron equilibrium is achieved if the active volume of the ionization chamber is surrounded by an infinite amount of equivalent air that is subject of the same exposure over the course of the measurement. Since this is not the case, the ionization chamber is constructed with air equivalent solid walls that are thicker than the maximum secondary electron range. Thus, the ionization lost from the active volume is compensated by ionization from secondary electrons created within the chamber walls. Both situations are illustrated in Figure 2.3.

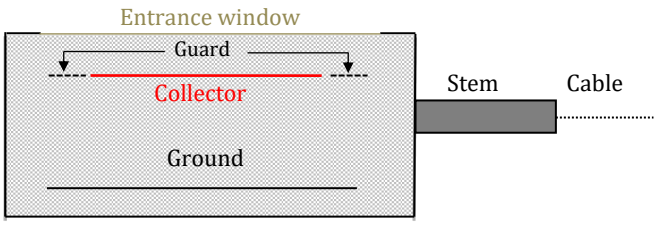

Figure 2.2: Internal structure of a typical plane parallel ionization chamber.

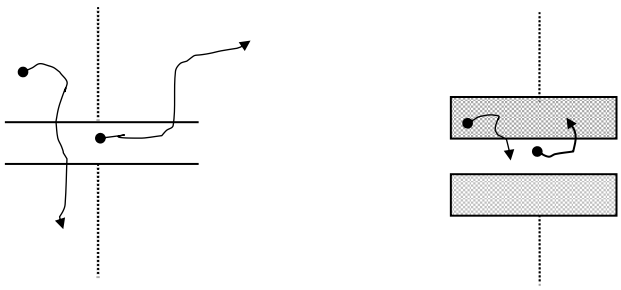

Figure 2.3: Left: ionization in free air. Right: chamber with air equivalent solid walls.

2.3.2 Semiconductor Dosimeters

Semiconductors are crystalline materials whose electrical conductivities are lower than those of metals but higher than those of insulators. In crystalline materials, electrons exist in energy bands, separated by gaps. In insulators and semiconductors at T=0 *K* the highest energy band containing electrons is completely occupied. This highest occupied band is the valence band, the band above the valence band is the conduction band. Since the valence band is fully occupied, electrons cannot move through the solid at T=0 *K*. For positive temperatures, the situation is different. There the band gap for semiconductors is about 1 *eV* and the thermal energy of some electrons is large enough to be lifted into the conduction band and move through the solid. For insulators the energy gap is about 10 *eV* therefore too large to promote electrons into the conduction band. Thus, semiconductors at finite temperatures conduct electric currents while insulators do not.

Their special band structure makes semiconductors adequate materials for the detection of ionizing radiation. When ionizing radiation interacts with a semiconductor, electrons are ionized. If those secondary electrons have enough energy, they will again ionize other atoms. In the case of ionizing photon radiation, the secondary electrons produce by far the largest part of

ionizations. In this way, several electrons get into the conduction band and can lead to a measurable current if a voltage is applied to the semiconductor. The electrons in the conduction band and the holes in the valence band correspond to the electron-ion pairs formed in ionization chamber. Since the amount of charge produced is proportional to the energy transferred by the primary radiation a signal proportional to the radiation absorbed can be produced.

A problem caused by impurities in semiconductors is, that they can act as electron and hole traps. Free electrons and holes generated by radiation hitting the detector can get caught by the energy states created by these impurities, which will diminish the ionization current caused by the radiation. By adding impurities to the semiconductor (doping) one can deliberately generate additional energy states within the gabs of forbidden energies. If the impurities generate energy states closer to the conduction band, there will be a greater number of electrons in the conduction band at positive temperature. These doped semiconductors are n-type semiconductors. If the impurities generate energy states lying closer to the valence band, electrons from the valence band can be excited to these states, leaving back holes in the valence band. These are p-type semiconductors. In n-type semiconductors most of the current is conducted by electrons, in p-type semiconductors by the holes.

Semiconductor detectors are mostly built in the form of semiconductor diodes. It consists of an n-type and a p-type semiconductor. The conduction properties of a diode depend on the direction in which the voltage is applied. Forward bias, positive voltage to the p-type and negative voltage to the n-type semiconductor, force the electrons from the n-type semiconductor to drift into the p-type semiconductor and the holes from the p-type vice versa into the n-type semiconductor. If the voltage is applied in the other direction (reverse bias), the conduction electrons and the holes are drawn back into the n-type and p-type semiconductors, thus creating a depletion zone, where no charge carriers are present. A semiconductor diode operated with reverse bias becomes effectively an insulator. The depletion zone around the n-p-junction is equivalent to the active volume of an ionization chamber. The generation of electron-hole pairs within the depletion zone by ionizing radiation leads to a current flowing through the otherwise insulating diode. The charge produced is proportional to the energy of the primary radiation.

Their sensitivity can be orders of magnitude higher than that of ionization chambers. Thus, the minimum air kerma required to produce a signal output is much lower. The energy dependence of the response of semiconductor dosimeters is more pronounced than that for ionization chambers [8]. Therefore, a variety of compensation methods were developed by the manufacturers to reduce this effect. There intrinsic energy dependence also makes them unsuitable for application in absolute dosimetry.

In addition to dose, semiconductor devices may provide also other quantities as dose rate, tube voltage and half-value layer (HVL) with one exposure. HVL is needed by the clinics to determine the mean glandular dose (see section 2.2) for quality assurance. Therefore and because they are easy to handle they are used more and more in clinical situations [8], [9].

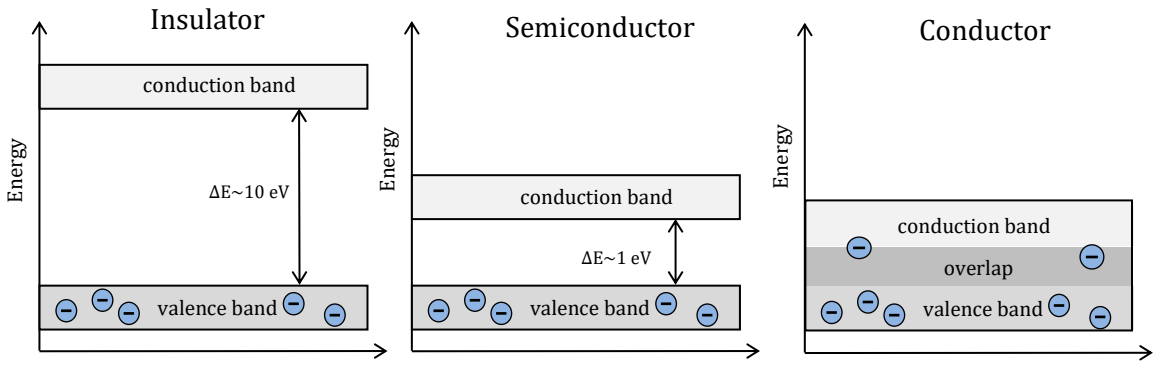

Figure 2.4: Electronic band structure of a solid.

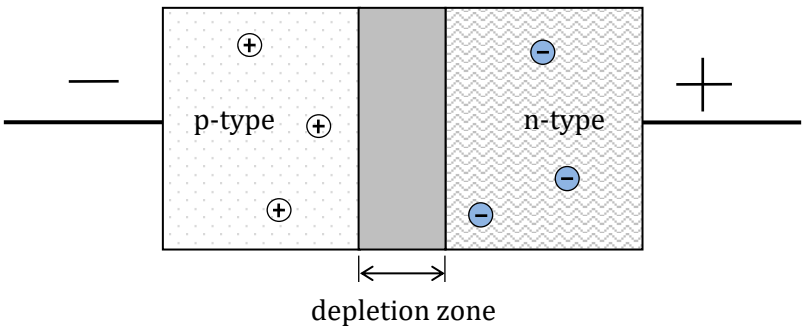

Figure 2.5: Scheme of a reverse-biased semiconductor diode. In the depletion zone are no free charges.

2.4 Calibration

The aim of calibration is to ensure that an instrument is working properly and hence will be suitable for its intended monitoring purpose. The Bureau International des Poids et Mesures (BIPM) defined calibration in the international vocabulary of metrology (VIM) as follows: "*Operation that, under specified conditions, in a first step, establishes a relation between the* ***quantity values*** *with* ***measurement uncertainties*** *provided by* ***measurement standards*** *and corresponding* ***indications*** *with associated measurement uncertainties and, in a second step, uses this information to establish a relation for obtaining a measurement result from an indication"*. A **quantity value** is a number with unit, together expressing the magnitude of a quantity. The **indication** is the quantity value provided by an instrument. The calibration factor is the relation of the quantity value provided by measurement standards (calibration coefficient in the certificate) together with the corresponding indication e.g. ionization current corrected for ambient conditions and the indication of the instrument to be calibrated [10].

To ensure that the measured dose all over the world is consistent it is necessary that the used dosimeters have a traceable calibration. Metrological traceability is a property of a measurement result whereby the result can be related to a reference (BIPM or Primary Standard Dosimetry Laboratory (PSDL)) through a documented unbroken chain of calibration. The BIPM and the PSDLs are on the top of this calibration hierarchy. Using a primary reference procedure, they are able to obtain a measurement result without relation to a measurement standard for a quantity of the same kind [10]. They employ free air ionization chambers for the measurements of air kerma traceable to the fundamental SI unit [*Gy*].

The most common way of calibrating dosimeters applied in diagnostic radiology is the substitution method. There, in the first step the reference value is determined by a reference class dosimeter traceable to measurement standards. Afterwards it is replaced by the dosimeter to be calibrated (user dosimeter) and the calibration factor of the user dosimeter can be determined.

2.4.1 International measurement system

The direct linkage of national dosimetry standards to the international measure standard traceable to the BIPM or another PSDL is provided by Secondary Standards Dosimetry Laboratories (SSDLs). The SSDLs calibrate their reference class instruments at PSDLs or at the IAEA and use these as their local dosimetry standards. Thus, the traceability of the measurements to the PSDL is maintained. For the confidence in this measurement system redundancy is essential. A robust method to guarantee this is to compare the standards against each other. A forum in which national SSDLs could perform these comparisons is the Network of SSDLs which was established in 1976 by the International Atomic Energy Agency (IAEA) together with the World Health Organization (WHO)[11].

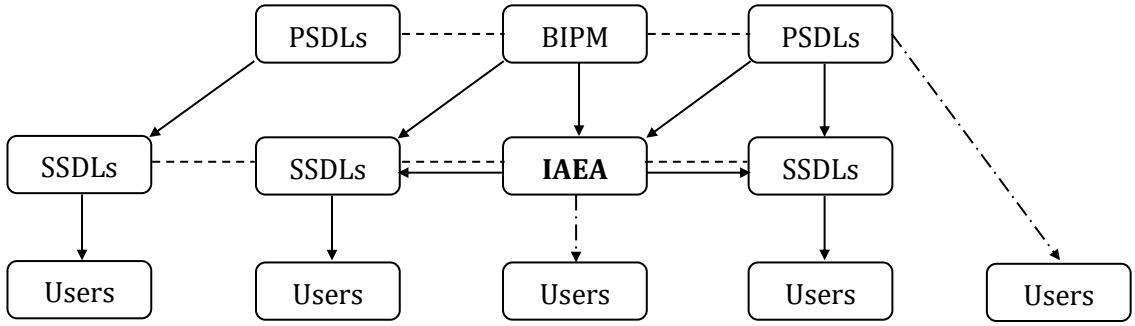

Figure 2.6: Schema of the international measurement system of radiation dosimetry. The arrows represent exchange of data (calibration), the dashed lines represent comparison and the dash dotted arrows indicates exceptional calibrations.

2.4.2 X-ray spectra

The production of X-rays involves the bombardment of a thick anode with high energetic electrons. The electrons are traveling from the cathode to the anode and are accelerated by the voltage applied. They attain kinetic energy equal to the product of the electrical charge and potential difference. On impact with the anode these electrons undergo a complex sequence of collisions and scattering processes. During the slowing down process the kinetic energy of the electrons is converted to electromagnetic radiation. This results in the continuous bremsstrahlung-spectrum and in characteristic lines. Characteristic lines are induced by electronic transitions between atomic shells following ionizations in the anode material. Their energy depends on the atomic number of the anode material. The unfiltered bremsstrahlung-spectrum has an inverse linear relationship between the number and energy of photons. The highest photon energy is determined by the peak voltage applied across the X-ray tube. The bremsstrahlung-spectrum is attenuated by the inherent filtration and the air between the X-ray tube and the point of measurement. Inherent filtration includes the attenuation of X-rays in the anode, tube envelope, exit port, insulating water and the window of the tube housing. Therefore, a typical filtered bremsstrahlung-spectrum has a lack of photons below 10 *keV*.

To adjust the spectrum for optimal imaging additional filtration is positioned in the beam path. By the passage of the beam through a layer of material low and high energy X-rays are removed selectively, dependent on the atomic number of the used material. Ideally, for mammography elements with K-absorption edge energies between 20 and 27 *keV* are employed. Mo, Rh and Ag fulfill this requirement, among others. The attenuation for the lowest X-ray energies is very high. It decreases as the X-ray energy increases up to the K-edge of the filter material. For energies just above the K-edge energy, the attenuation increases as a step function as photoelectric absorption increases dramatically for this energy. At higher energies, the attenuation decreases.

An unfiltered and filtered bremsstrahlung-spectrum is displayed in the left subfigure of Figure 2.7. The right subfigure shows the spectrum of a Mo-anode with 30 *kV* tube voltage (solid line) and the attenuation of Mo as a function of energy (dashed line) [8], [9].

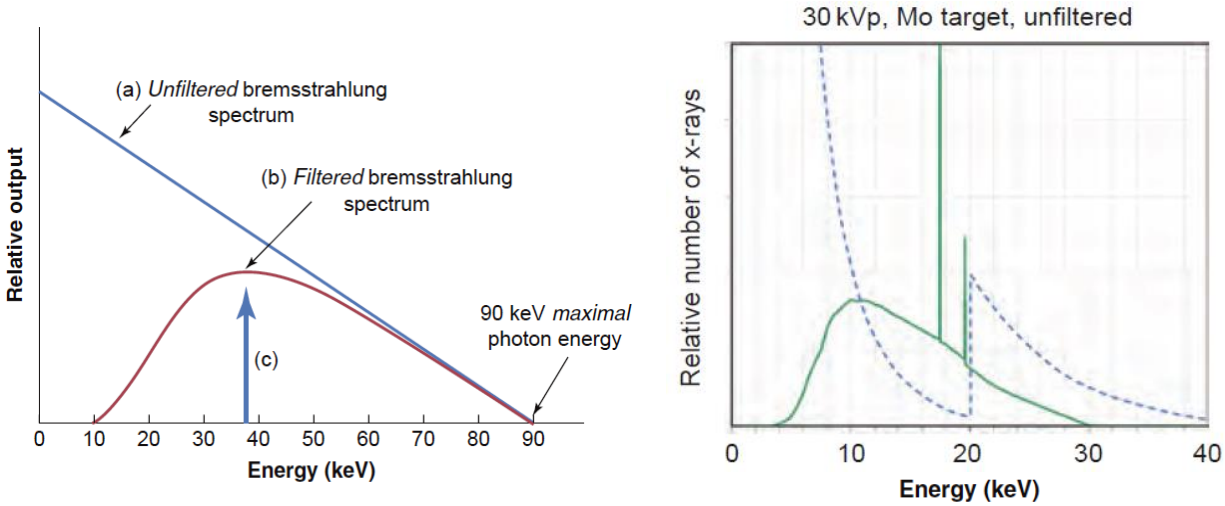

Figure 2.7: Left: Bremsstrahlung energy distribution (tube voltage 90 *kV*). (a) Greater probability of low-energy X-ray photon production. (b) Preferential attenuation of the low energy X-rays by the inherent filtration. Blue arrow (c): average energy of the spectrum.
Right: Solid line: unfiltered spectrum of a Mo-anode with 30 *kV* tube voltage. Dashed line: attenuation of a Mo filter as a function of energy. Both from [9].

2.4.3 Half-value layer

The common quantity to specify the spectrum with just one parameter is represented by the half value layer (HVL). The first HVL is defined as the thickness of a specific material required to reduce the air kerma of an X-ray beam to one half of its initial value as described in equation (2.4). μ corresponds to the linear attenuation coefficient and I_0 to the incident intensity. In diagnostic radiology dosimetry usually, aluminum is chosen as attenuator. Thus, the unit of HVL is *mm Al*. The HVLs of mammographic X-ray beams are listed in Table 3.1.

$$\frac{I_0}{2} = I_0 e^{-\mu(1.HVL)} \qquad (2.4)$$

To measure the HVL the air kerma is determined without and with additional layers of aluminum in the beam. It is plotted as a function of thickness of attenuators and the result is derived by interpolation from the graph. The experimental set-up as recommended by [12] is shown in Figure 2.8. If scattered photons are excluded from being detected, the HVL is an indirect measure of the mean photon energy of the beam. To reduce the number of scattered photons detected, the aperture in the beam limiting diaphragm should be just large enough to produce the smallest beam for complete and uniform irradiation of the ionization chamber. Further, the absorbers should be located equidistant from the monitor chamber and the detector. To eliminate the effects of variation of the X-ray tube output the readings of the ionization chamber should be normalized to the readings of the monitor chamber. In general, the HVL increases with higher tube voltages and higher atomic number of anode and filters [9], [12].

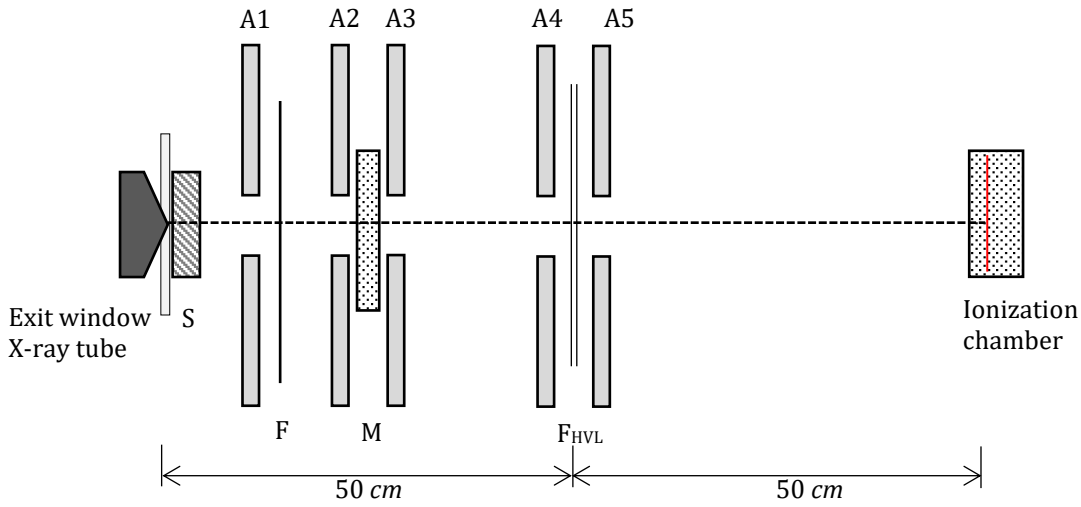

Figure 2.8: Scheme of HVL measurement set up. S: Shutter, F: Filtration, M: Monitor chamber, F_{HVL}: HVL absorber, A1-A5: Apertures.

2.4.4
Radiation qualities in clinical mammography

There are various anode-filter combinations in clinical use dependent on the manufacturers. The most common are listed in Table 2.1. In addition, it should be considered that a compression paddle of unspecified material and thickness is in the beam for clinical mammography since absorption of the lower energy photons affects the radiation quality. This variation has a direct impact on the calculation of the mean glandular dose.

Table 2.1: Typical anode-filter combinations for clinical mammography [13]–[19].

Anode	Filtration	Manufacturer
Mo	0.03 *mm* Mo	Eco-Ray, Fujifilm, GE, Giotto, Hologic, Planmed, Siemens
	0.025 *mm* Rh	Fujifilm, GE, Giotto, Hologic, Planmed, Siemens
Rh	0.025 *mm* Rh	GE
W	0.3 - 0.7 *mm* Al	Hologic, Philips, Sectra
	0.05 or 0.06 *mm* Rh	Fujifilm, Giotto, Hologic, MS Westfalia, Planmed, Siemens
	0.05 - 0.075 *mm* Ag	Giotto, Hologic, Planmed
	0.3 *mm* Cu	Hologic

2.4.5
Radiation qualities for calibration

The calibration of diagnostic radiology dosimeters should be performed with radiation qualities described in the Norme Internationale CEI/IEC 61267:2005 [12] [1]. There, the standard radiation conditions for calibration of dosimeters used for mammography are defined. All of them are produced by an X-ray tube with molybdenum anode and molybdenum filter. For RQN-M and RQB-M radiation qualities a phantom is used as additional filtration. This phantom is made of 45 *mm* polymethylmethacrylate (PMMA) with the purpose of simulating a breast of 50% adipose and 50% glandular tissue. However, these phantom related qualities are rarely used.

Table 2.2: Radiation qualities for mammography defined in IEC 61267 [1].

Radiation Quality	**Filtration**	**Tube voltage in *kV***	**1. HVL in *mm* Al**
Anode material molybdenum			
RQR-M	0.032 *mm* Mo	25 - 35	0.28 - 0.36
RQA-M	0.032 *mm* Mo, 2 *mm* Al	25 - 35	0.56 - 0.68
RQN-M	0.032 *mm* Mo, Phantom, narrow beam condition	25 - 35	0.37 - 0.70
RQB-M	0.032 *mm* Mo Phantom, broad beam condition	25 - 35	–

The Bureau International des Poids et Mesures (BIPM) maintains primary standards of air kerma and absorbed dose that are used as international reference standards. The radiation qualities listed in Table 2.3 are established for X-rays of 10 *kV* to 50 *kV* at BIPM [20]. The Physikalisch-Technische Bundesanstalt (PTB), established the radiation qualities listed in Table 2.4 for mammography. PTB and BIPM employ a free air ionization chamber as a primary standard [21].

Table 2.3: Radiation qualities for X-rays (10 *kV* to 50 *kV*) established by BIPM [20].

Anode material	**Filtration**	**Tube voltage in *kV***	**1.HVL in *mm* Al**
Mo	0.03 *mm* Mo	25 - 35	0.277 - 0.365
W	0.06 *mm* Mo	23 - 50	0.332 - 0.489

Table 2.4: Radiation qualities for mammography established by PTB. All listed qualities are also available as attenuated qualities (additional filtration of 2 *mm* Al) [21].

Anode material	**Filtration**	**Tube voltage in *kV***	**1.HVL in *mm Al***
Mo	0.03 *mm* Mo	20 - 50	0.22 - 0.43
	0.025 *mm* Rh	20 - 50	0.24 - 0.48
	1 *mm* Al	20 - 50	0.34 - 0.67
Rh	0,025 *mm* Rh	20 - 50	0.24 - 0.56
	1 *mm* Al	20 - 50	0.34 - 0.85
W	0.5 *mm* Al	20 - 50	0.26 - 0.70
	0.7 *mm* Al	23 - 35	0.34 - 0.64
	0.05 *mm* Rh	20 - 50	0.35 - 0.71
	0.05 *mm* Ag	20 - 50	0.35 - 0.79
	0.06 *mm* Mo	20 - 50	0.31 - 0.56
	0.04 *mm* Pd	20 - 50	0.32 - 0.69

2.4.6
Dosimetry formalism

The air kerma K_{air} at the reference point in air for a reference beam quality Q_0 in the absence of a dosimeter is given by

$$K = \left(M_{Q_0} - M_0\right) N_{K,Q_0} \prod_i k_i^{ref} \,. \tag{2.5}$$

M_{Q_0} represents the reading of the dosimeter under reference conditions and M_0 is the leakage, the reading in the absence of radiation. N_{K,Q_0} is the calibration coefficient of the dosimeter in terms of the air kerma provided by measurement standards (calibration laboratories). Since the calibration coefficient refers to defined reference conditions corrections for measurement conditions are necessary. Reference conditions are a set of influence quantities which are not subject of the measurement but have an influence on the result. Influence quantities act independently therefore their correction $\prod_i k_i^{ref}$ is the product of the individual correction for each influence quantity. For measurements with ionization chambers a correction for the density of air in the active volume $k_{T,P}$ is necessary. It allows for temperature T and pressure P different from the reference temperature T_0 and pressure P_0. Further correction factors are not applied to the calculation of air kerma but considered in the uncertainty budged (see section 4.7).

$$k_{T,P} = \left(\frac{273{,}2 + T}{273{,}2 + T_0}\right)\left(\frac{P_0}{P}\right) \tag{2.6}$$

The calibration factor N_{K,Q_0}^{user} is obtained from the air kerma K prevailing at the point of test and the instrument`s indication $M_{Q_0}^{user}$.

$$N_{K,Q_0}^{user} = \frac{K}{M_{Q_0}^{user}} \tag{2.7}$$

The indications provided by the dosimeters can be of different kind. As discussed in sections 2.3.1 and 2.3.2 the signal which results from the impact of radiation on the detector is electrical current. While the reading obtained by ionization chambers is this ionization current directly it is impossible to get the resulting ionization current out of a semiconductor dosimeter. Thus, the indications of semiconductor dosimeters include an inherent calibration factor.

A general approach is, instead of giving the calibration factor N_{K,Q_0} for all radiation qualities, to state the calibration factor in the calibration certificate for the standard radiation quality Q_0 and a correction factor k_q for all other radiation qualities.

$$k_q = \frac{N_q}{N_{Q_0}} \tag{2.8}$$

2.4.7
Calibration Scenarios

One scenario is that the reading of the semiconductor dosimeter is used directly with internal calibration and no additional calibration factors are applied. In the second scenario, the calibration factor for one radiation quality is available. Therefore, the indication is corrected for the standard radiation quality but the correction k_q to other radiation qualities is missing.

Usually, calibration is performed without compression paddle or any other material to simulate the compression paddle, in the beam. For this study a compression paddle was simulated by additional PMMA. To determine the error $Error_{PMMA}$ occurring, the calibration factor determined with additional PMMA N_q(PMMA) is normalized to the calibration factor without PMMA($N_q(0)$) for the same radiation quality.

$$Error_{PMMA} = \frac{N_q(PMMA)}{N_q(0)} \tag{2.9}$$

2.5 Objective

This thesis presents a test of eight semiconductor dosimeters and one ionization chamber under calibration conditions in the IAEA Dosimetry Laboratory. Five different radiation qualities were used covering the mostly common anode-filter combinations in clinical mammography units (W-Al, W-Rh, W-Ag, Mo-Mo and Mo-Rh) and a tube voltage range from 25 to 35 *kV*. Further, the effect of additional filtration of different thicknesses of PMMA in the beam was investigated. To estimate the maximum error which can occur if the appropriate radiation quality for calibration is not available the built-in compensation of the energy dependence of the response was determined.

In the past, manly radiation qualities with Mo-anode and Mo-filtration were used for film screen mammography. Therefore, only this radiation quality is considered in the International Standard 61267 [1] for calibration of mammography equipment. Nowadays, for digital mammography a wide range of radiation qualities is used. For calibrating ionization chambers a variation of radiation quality is not an issue. The energy dependence of their response is negligible. For semiconductor dosimeters the situation is different. The energy dependence of their response is more pronounced than that of ionization chambers.

Normally, SSDLs are equipped with W-anodes. Mo-anodes are not available everywhere. Additional, there is a lack of information and guidance for SSDLs how to deal with semiconductor dosimeters. For the independence of many countries it is necessary that the national SSDL can perform the calibration in the country. The IAEA dosimetry laboratory was chosen for this large scaled test because of the availability of a secondary standard, traceable to the PSDL for the chosen radiation qualities.

The energy dependence of the response of semiconductor dosimeters in the range of clinical X-ray radiation qualities may be significant. To improve the performance of the semiconductor dosimeters manufacturers developed several compensation methods which often require a preselection of the radiation quality used or whether a compression paddle is in the beam or not. Differences between calibration and clinical radiation qualities occur in the terms of applied air kerma rate, anode-filter combination, tube voltage and additional filtration by a compression paddle of unknown composition and thickness. The compression paddle affects the HVL of the radiation which is necessary to calculate the mean glandular dose.

The effect of the radiation quality on the performance of semiconductor dosimeters was shown by previous studies. Brateman and Heintz in 2015 found differences in air kerma measurements on clinical mammography units for semiconductor dosimeters from -6% to +7% compared with air kerma measured by ionization chambers. Brateman and Heintz found that the HVL and air kerma measurement with semiconductor dosimeter on clinical mammography units leads to an underestimation of mean glandular dose with discrepancies of -1% to -10%. Sekimoto et all in 2015 tested two semiconductor dosimeters and three ionization chambers for six different anode-filter combinations with additional filtration of 3 *mm* PMMA to investigate the effect of the radiation quality on the calibration factor. The maximum error they found was +33% [22] [23].

3 Material and Methods

3.1 Irradiation facility

The X-ray tube types Isovolt MXR-160 and MCD 100H-5 Mo were used to generate radiation qualities with W- and Mo-anodes, respectively. The output of the high-voltage generator, type ISOVOLT 160 Titan E is monitored using a high-voltage divider, type FUG HVT 160 000. This high-voltage divider was calibrated at PTB.

3.2 IAEA radiation qualities

Radiation qualities defined in the IAEA Appendix 2 DOLP.013 [24] are available at the IAEA dosimetry laboratory (see Table 3.1). They were established by setting the correct high voltage and measuring the 1st (and 2nd half-value) layer. For simulating the compression paddle, which is in the beam for clinical use, additional radiation qualities were established. The first HVL for these modified radiation qualities are listed in Table 3.2.

Table 3.1: Radiation qualities for mammography established in the IAEA dosimetry laboratory.

Radiation Quality	**Filtration**	**Tube voltage in *kV***	**1.HVL in *mm* Al**	**Source of traceability**
Mo-Mo	0.033 *mm* Mo	25 - 35	0.289 - 0.344	BIPM
Mo-Rh	0.0285 *mm* Rh	28 - 35	0.393 - 0.446	PTB
Mo-Mo-Al	0.033 *mm* Mo 2.020 *mm* Al	25 - 35	0.582 - 0.730	PTB
W-Al	0.5 *mm* Al	25 - 35	0.312 - 0.435	PTB
W-Rh	0.0477 *mm* Rh	25 - 35	0.469 - 0.549	PTB
W-Ag	0.0492 *mm* Ag	25 - 35	0.487 - 0.605	PTB
W-Mo	0.066 *mm* Mo	25 - 35	0.340 - 0.393	BIPM

Table 3.2*:* PMMA attenuated radiation qualities established in the IAEA dosimetry laboratory.

Radiation Quality	**Tube voltage in *kV***	**1.HVL in *mm* Al for additional PMMA**			
		0 *mm*	**1.968 *mm***	**2.775 *mm***	**4.761 *mm***
Mo-Mo	25	0.289	0.327	0.345	0.377
	28	0.324	0.364	0.380	0.404
	30	0.344	0.388	0.398	0.426
	35	0.381	0.421	0.434	0.463
W-Al	25	0.312	0.371	0.389	0.427
	28	0.354	0.413	0.437	0.488
	30	0.380	0.452	0.477	0.527
	35	0.435	0.519	0.550	0.614

3.2.1
Establishment of modified radiation qualities

The determination of the HVL was performed according the Technical Report Series No. 457 [12]. A scheme of the measurement set-up is shown in Figure 3.1. The ionization chamber was placed at 1 *m* distance to the focal spot. The beam limiting diaphragm including the Al sheet was positioned equidistant between the X-ray beam exit window and the ionization chamber. The diaphragm had a diameter of 2.5 *cm* which leads to a beam diameter of 6 *cm* at the point of test. The additional PMMA sheets were placed after the monitor chamber. To avoid differences caused by variation in the output of the X-ray tube the readings of the ionization chamber were normalized to the monitor chamber. First, the reference air kerma rate in the absence of any absorber was determined afterwards with different absorber thicknesses. The measured air kerma rate for various absorber thicknesses were plotted versus the absorber thickness on a semi-logarithmic scale. The HVL values were derived by linear interpolation from the graph using three points near to the estimated value. The determined HVLs are listed in Table 3.2.

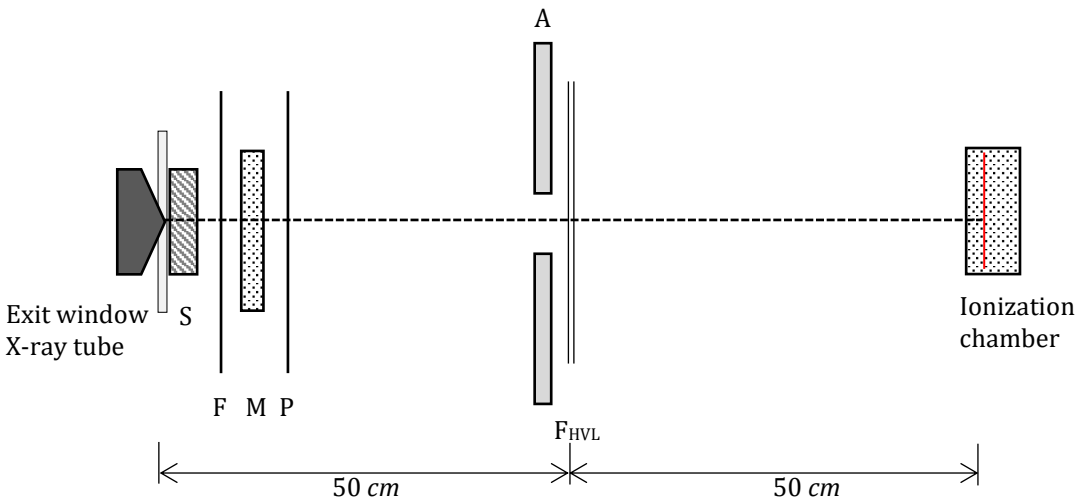

Figure 3.1: Scheme of the HVL measuring set-up. S: Shutter, F: Filtration, M: Monitor chamber, P: PMMA filtration, A: Aperture, F_{HVL}: HVL absorber.

3.3
Reference standard

The reference standard for this study is a Radcal 10X5-6M ionization chamber. This chamber is a working standard of the IAEA dosimetry laboratory. The traceability of its calibration factors in dependence of the radiation quality is listed in Table 3.1. The energy response over the range of radiation qualities used for mammography is extraordinary flat and the response is not significantly influenced by the anode material or filtration.

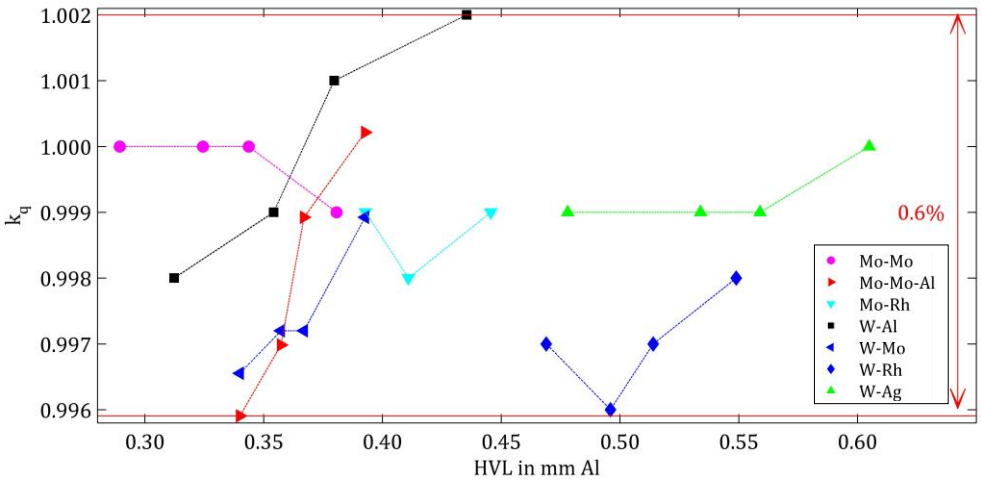

Figure 3.2: Correction factor k_q of the reference standard ionization chamber 10X5-6M normalized to the standard radiation quality Mo-Mo 28 as a function of half-value layer (HVL).

Table 3.3: Specification of the reference standard ionization chamber 10X5-6M according to the specification sheet [25].

Active detector		**Range**		**Energy dependence**	**Entrance window**
Depth[1]	**Volume**	**Dose**	**Dose Rate**		
8.4 *mm*	6 cm^3	0.01 μGy - 600 *Gy*	0.1 $\mu Gy/s$ - 7400 *mGy/s*	±5%[2], 10 *keV* to 40 *keV*	0.7 mg/cm^2 metalized polyester

3.4
User dosimeters

The dosimeters listed in Table 3.4 were calibrated for this study. Eight semiconductor dosimeters and one ionization chamber were chosen. Each of them was regularly quality controlled. Their specifications according to the manuals are listed in Table 3.5 and those for quantities of interest in Table 3.6. For all semiconductor dosimeters (except the Unfors X2) it is necessary to select the applied radiation quality in the software. The Unfors X2 dosimeter only requires this selection for measurement of tube voltage. For determining the calibration factor N_{K,Q_0}^{user} as described in formula (2.7) the air kerma rate was used exclusively. HVL and tube voltage measurement capabilities were tested additionally for those dosimeters which have this possibility. Available selections of radiation qualities and the provided indications are listed in Table 3.7.

[1] Below the polyacetal exterior
[2] The measured energy dependence is much lower.

Table 3.4*:* Dosimeters calibrated in this study.

Manu-facturer	Detector assembly	Measuring assembly	Manual	Software
RTI	Internal detector	Piranha 657	[26]	Ocean, Version: 2010.12.15.38
RTI	R100B[3]	Barracuda	[27]	Ocean, Version: 2010.12.15.38
Unfors	Mult-O-Meter		[28]	Display read directly
RTI	Internal detector	Black Piranha	[29]	Ocean, Version: 2016.06.14.214
Unfors	MAM	Xi	[30]	RaySafe Xi View, Version: 3.0 (built 47)
PTW	Internal detector	Nomex Multimeter	[31]	Nomex Software S030008, 3.0
Radcal	AGMS –DM+	Accu Gold	[32]	Accu-Gold by Radcal, Version 1.5.3.0 Driver Version 02.10.00
Unfors	MAM	X2	[33][34]	RaySafe X2 View, Version 1.7.8.0
PTW	M77334[4]	Kethley6517A	[35]	Data acquisition system of the IAEA DOL developed in LabVIEW

Table 3.5: Specifications of the user dosimeters according to the manuals.

Measuring assembly	Active detector		Range			
	Depth in *mm*	Area in cm^2 or volume* in cm^3	Dose in *µGy-Gy*	Dose Rate in *µGy/s-mGy/s*	HVL in *mm* Al [5]	Tube voltage in *kVp* [5]
Piranha 657	10	0.63	5 - 1500	10 - 750	—	18 - 40
Barracuda	3	1	0.0001 - 1500	0.004 - 76	—	—
Mult-O-Meter	8.5	1.05	0.001 - 9999	100 - 500	—	—
Black Piranha	10	0.63	5 - 1000	10 - 530	0.19 - 0.69	18 - 40
Xi	7	0.8	5 - 9999	10 - 100	0.2 - 1.2	20 - 49
Nomex	4.7	18.4	0.5 - 500	50 - 500	0.25 - 0.75	23 - 35
Accu Gold	3.2	0.76	0.15 - 100	0.15 - 350	0.16 - 0.82	20 - 50
X2	3	0.05	1 - 9999	10 - 300	0.2 - 3.6	20 - 40
M77334	2.3	1*	1 *mGy* [6] [7]	17000 *Gy/s* [6]	—	—

[3] Not recommended by the manufacturer for mammography since no automatic compensation is available.
[4] Ionization Chamber
[5] Ranges for different radiation qualities are specified in the manual
[6] 99% saturation
[7] Max dose per pulse

Table 3.6: Specifications for quantities of interest according to the manuals.

Measuring assembly	**Dose rate**[8]	**HVL**	**Tube voltage**
Piranha 657	±5% or ±12 nGy/s [9]	—	±2% or ±1 kV, for Mo-Mo ±1.5% or±0.7 kV[9]
Barracuda- R100B	±5% or ±1 nGy/s [9]	—	—
Mult-O-Meter	±5% for 25-30 kVp range	—	—
Black Pirnaha	±5%	±10%	±2% or ±1 kV, for Mo-Mo ±1.5% or±0,7 kV [9]
Xi	±5% or ±5 $\mu Gy/s$ [9]	±5%	±2% or ±0.5 kV [9] (no CP)
Nomex	±2.5%	±0.01 mm Al	±0.5 kV
Accu Gold	±5%	±10% or ±0.05 mm Al [9]	±2% or ±0.7 kV [9]
X2	±5%	±5%	±2% or ±0.5 kV [9] (no CP)
M77334	—	—	—

Table 3.7: Available calibrations and indications of the user dosimeters.

Measuring assembly	**Calibration in the software** [10]					**Indications**		
	W-Al	**W-Rh**	**W-Ag**	**Mo-Rh**	**Mo-Mo**	**Dose Rate**	**HVL**	**Tube voltage**
Piranha 657	×	×	×	×	×	×	—	×
Barracuda	—	—	—	—	×	×	—	—
Mult-O-Meter	—	—	—	—	×	×	—	—
Black Piranha	×	×	×	×	×	×	×	×
Xi	×	×	×	×	×	×	×	×
Nomex	×	×	×	×	×	×	×	×
Accu Gold	—	×	×	×	×	×	×	×
X2	×	×	×	×	×	×	×	×

3.5

Measurement set-up

The reference ionization chamber and the user dosimeter are placed free in air on the calibration bench. The movement of the cart, perpendicular to the beam, is digitally controlled to ensure the reproducibility of the positioning. Under the guidance of a laser system, the reference point of both dosimeters is placed perpendicular to the central axis of the beam. The distance from the focus of the X-ray tube to the reference point of the dosimeter is 100 cm. The reference point is specified by the manufacturer and listed in Table 3.5. The distance is determined with a telescope and a mark on the wall. First the reference dosimeter is in the beam and at least 3 readings each 10 s are taken. Afterwards the reference dosimeter is substituted by the user dosimeter by moving the cart on the calibration bench. Again, at least 3 readings each 10 s are taken. To determine the short-term repeatability the standard deviation is calculated for each

[8] The International Standard 61674 requires limits of variation of ±5% for reference conditions.
[9] Whichever is greater.
[10] In several dosimeters further calibrations are available.

set of 3 readings. The reference dosimeter is connected to a Keithley 6517A electrometer and the data acquisition system of the IAEA DOL developed in LabVIEW. A pre-irradiation of the chamber is started to achieve electrical equilibrium in the chamber before starting the calibration measurements [36].

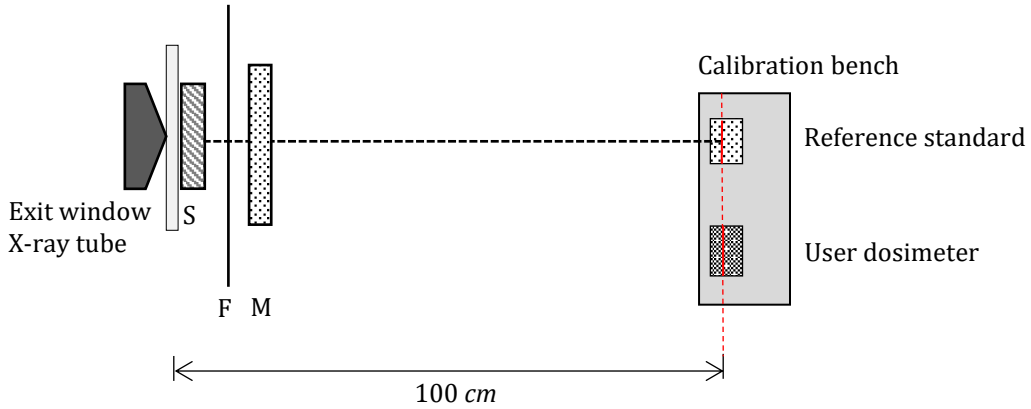

Figure 3.3: Set up for calibration with the substitution method. S: Shutter, F: Filtration, M: Monitor chamber, Red dashed line: point of test and reference plane of the dosimeters.

3.6
Determination of the reference value

The Technical Report Series No. 457 [12] recommends to use a plane parallel ionization chamber, with a maximum variation of energy response of ±2.6% and a range of air kerma rate measurement of 10 $\mu Gy/s$ - 10 mGy/s, as a reference class dosimeter. The specifications of the used reference class dosimeter, Radcal 10X5-6M, are listed in Table 3.3. The variation of energy response is 0.6% and much lower than stated in the specification sheet and recommended by the Technical Report Series No. 457.

The air kerma rate $\dot{K}_{\text{air}}\,[mGy/s]$ is determined by multiplying the ionization current I $[pA]$ with the calibration coefficient $N_k\,[mGy/nC]$ provided by the measurement standards (PSDL). The calibration coefficient refers to T=20 $°C$, P=101.325 kPa and 50% humidity. Therefore, a correction factor for the actual air density $k_{T,P}$ (equation (2.6)) is applied.

$$\dot{K}_{air}[mGy/s] = I_{norm}[pA] * k_{T,P} * N_k[mGy/nC] \qquad (3.1)$$

To normalize the ionization current to the reading of the monitor chamber it is multiplied with the ratio of the indication of the monitor chamber read simultaneously with the user dosimeter m_2 and the indication of the monitor chamber read simultaneously with the reference standard m_1.

$$I_{norm}[pA] = I[pA]\frac{m_2}{m_1} \qquad (3.2)$$

3.7
Determination of the calibration factor of the user dosimeter

The dimensionless calibration factor N of the user dosimeter is the ratio of the air kerma rate $\dot{K}_{\text{air}}\,[mGy/s]$ obtained with the reference standard, and the reading $\dot{M}_{\text{air}}\,[mGy/s]$ of the user dosimeter (equation (3.3)). According to the different operating modes of the user dosimeters there were two ways to normalize the reference value to the monitor chamber reading. Either using the timed measuring mode or use the timing by the built-in trigger. The Piranha 657, Barracuda and Black Piranha were operated in timed mode where the measurements were

started and stopped by the software and the shutter was open all the time. Thus, the monitor chamber was read simultaneously, and the ionization current of the reference dosimeter was normalized according to equation (3.2). All other user dosimeters (except the ionization chamber) were timed by their built-in trigger and the measurement was started and stopped by opening and closing the shutter. In this case, the reference dosimeter was read right before (index b) and after (index a) the user dosimeter, and the average of both readings was taken.

$$N = \frac{\dot{K}_{air}[mGy/s]}{\dot{M}[mGy/s]} \tag{3.3}$$

$$I_{norm}[pA] = \frac{1}{N}\left(\sum_{b=1}^{n} I_b + \sum_{a=n+1}^{N} I_a\right) \tag{3.4}$$

3.8

Determination of the built-in correction of the user dosimeters

To investigate the built-in correction of the energy dependence of the response measurements with wrong selected radiation quality in the software were performed. For each radiation quality applied, calibration factors for different selections of the radiation quality were determined. Some manufacturers specify the thickness of filtration of the selectable radiation quality in the manual. With one exception, the thickness of filtration of the selected and applied radiation quality matches. Accu Gold specifies the calibration for W-Al with a filtration of 0.7 *mm* Al, which is 0.2 *mm* Al more filtration than for the applied radiation quality. Therefore, this selection was treated as wrong, even the anode-filter combination was the same. The available selections for all tested dosimeters are listed in Table 3.7. The calibration factors were determined in a similar way as described in section 3.7. k_q is the ratio of the air kerma rate and the air kerma rate for the standard radiation quality Mo-Mo 28 obtained with appropriate selection of the radiation quality in the software.

4 Results

4.1 Calibration factors for air kerma rate

The range of calibration factors *N* as a function of HVL of all dosimeters tested is shown in Figure 4.1. The vertical lines connect minimum and maximum values of all dosimeters tested for every radiation quality used. For better visualization minimum and maximum values, respectively, for each anode-filter combination, are connected.

Figure 4.2 shows the range of all dosimeters tested for their energy dependence of the response in terms of correction factors k_q to the standard radiation quality Mo-Mo 28. The circle in each box is the median, the edges of the boxes are the 25th and 75th percentiles. The whiskers extend to the minimum and maximum value. The red horizontal lines are the range of k_q for the reference standard ionization chamber. The black lines are the ±5% limit of variation for the effect of an influence quantity recommended by the international standard IEC 61674 [2]. The detailed data are listed in the appendix. Table 4.1 presents the maximum error of measurements without applied calibration factor and with calibration factor for one radiation quality as discussed in 2.4.7.

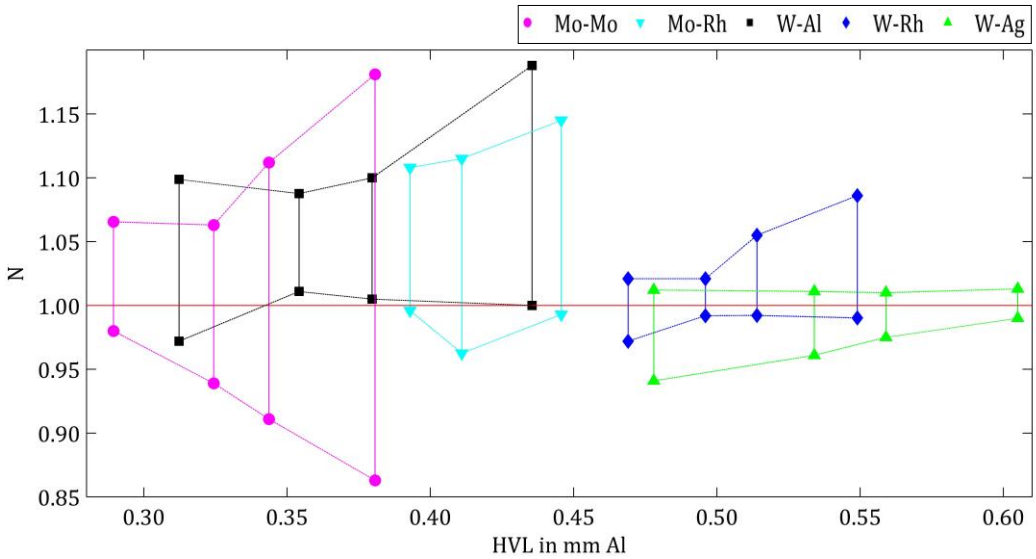

Figure 4.1: Range of calibration factors *N* for all user dosimeters as a function of HVL.

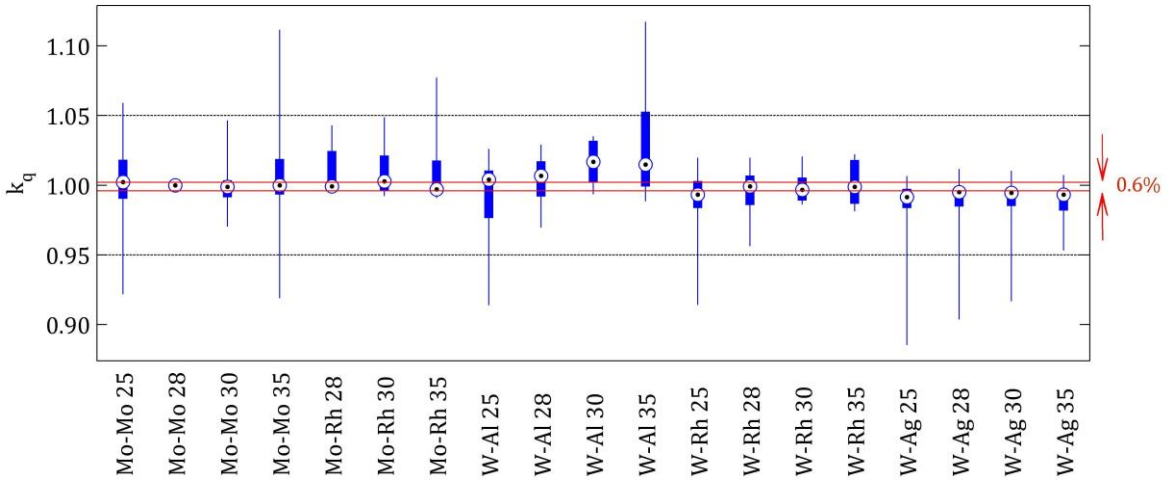

Figure 4.2: Range of all tested dosimeters for the correction factor k_q for the radiation quality Mo-Mo 28.

Table 4.1: Errors in % which occur if no calibration or one calibration factor is applied.

Measuring Assembly	Maximum error %	
	No calibration	Calibration with Mo-Mo 28
Piranha 657	16	-13
Barracuda, R100B	-16	-9
Mult-O-Meter	6	5
Black Piranha	4	3
Nomex	9	8
Xi	3	3
Accu Gold, AGMS-DM+	1	-2
X2	3	2
M77334	—	1

4.2 Calibration of air kerma rate under modified conditions

To investigate the connection of the energy dependence of the response with the spectra, four dosimeters were calibrated for W-Al and Mo-Mo with additional filtration of PMMA. Black Piranha, Nomex and X2 have the option to select the use of a compression paddle in the software. However, this choice is not available for the X2 with the radiation quality W-Al. Calibration was performed in both modes with modified radiation qualities (see section 3.2.1). The range of the calibration factors N and correction factors k_q are listed in Table 4.2. The correction factor k_q is determined as the ratio of the calibration factor N for each radiation quality and each thickness of PMMA and the calibration factor N for Mo-Mo 28 without additional PMMA and selection “no compression paddle” in the software, if available. Figure 4.3 (a) to (e) show the correction factors k_q determined under these modified conditions. The occurring error in this measurement scenario is determined according to equation (2.9).

Table 4.2: Range of calibration factor *N* and for calibration under modified conditions and the maximum occurring error in this calibration scenario.

	***N* for W-Al**		***N* for Mo-Mo**		**Error %**
CP selected in software	**no**	**yes**	**no**	**yes**	
Barracuda, R100B	0.97 - 0.69	×	1.0 0.75	×	11
Black Piranha	1.02 - 0.90	1.06 - 0.94	1.02 - 0.92	1.05 - 0.95	7
Nomex	1.01 - 1.01	1.13 - 1.02	1.03 - 0.97	1.05 - 0.99	6
X2	1.02 - 0.98	×	1.01 - 0.99-	1.01 - 0.99	0
M77334	24.3 - 23.9	×	24.3 - 24.0	×	1

(a) Barracura, R100B

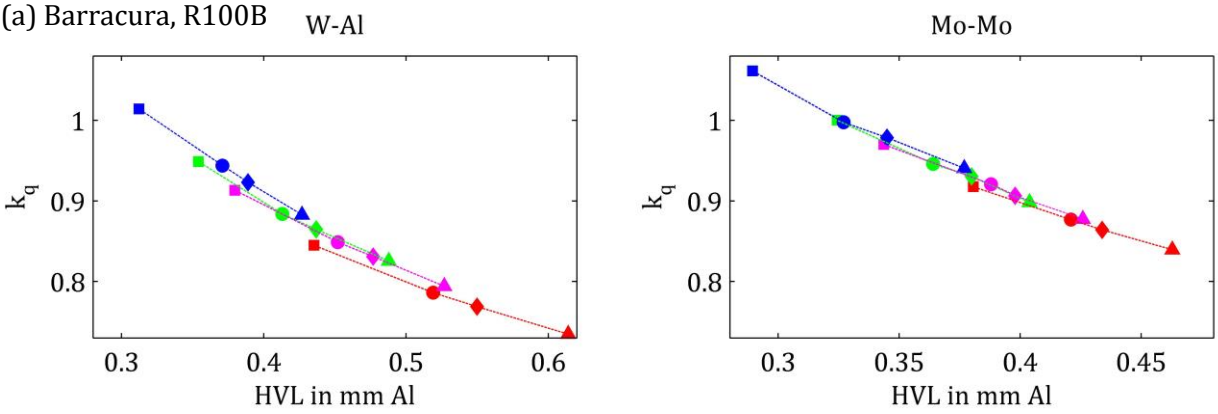

(b) Black Piranha

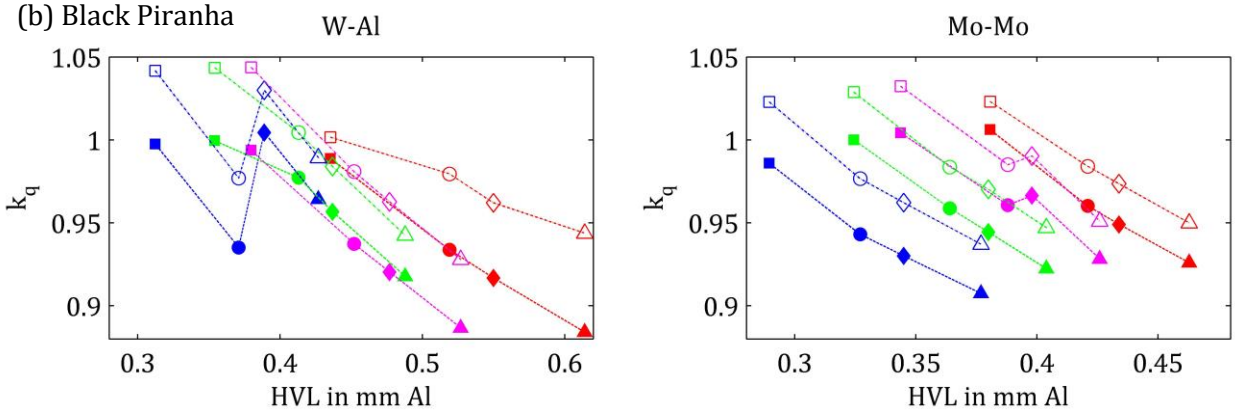

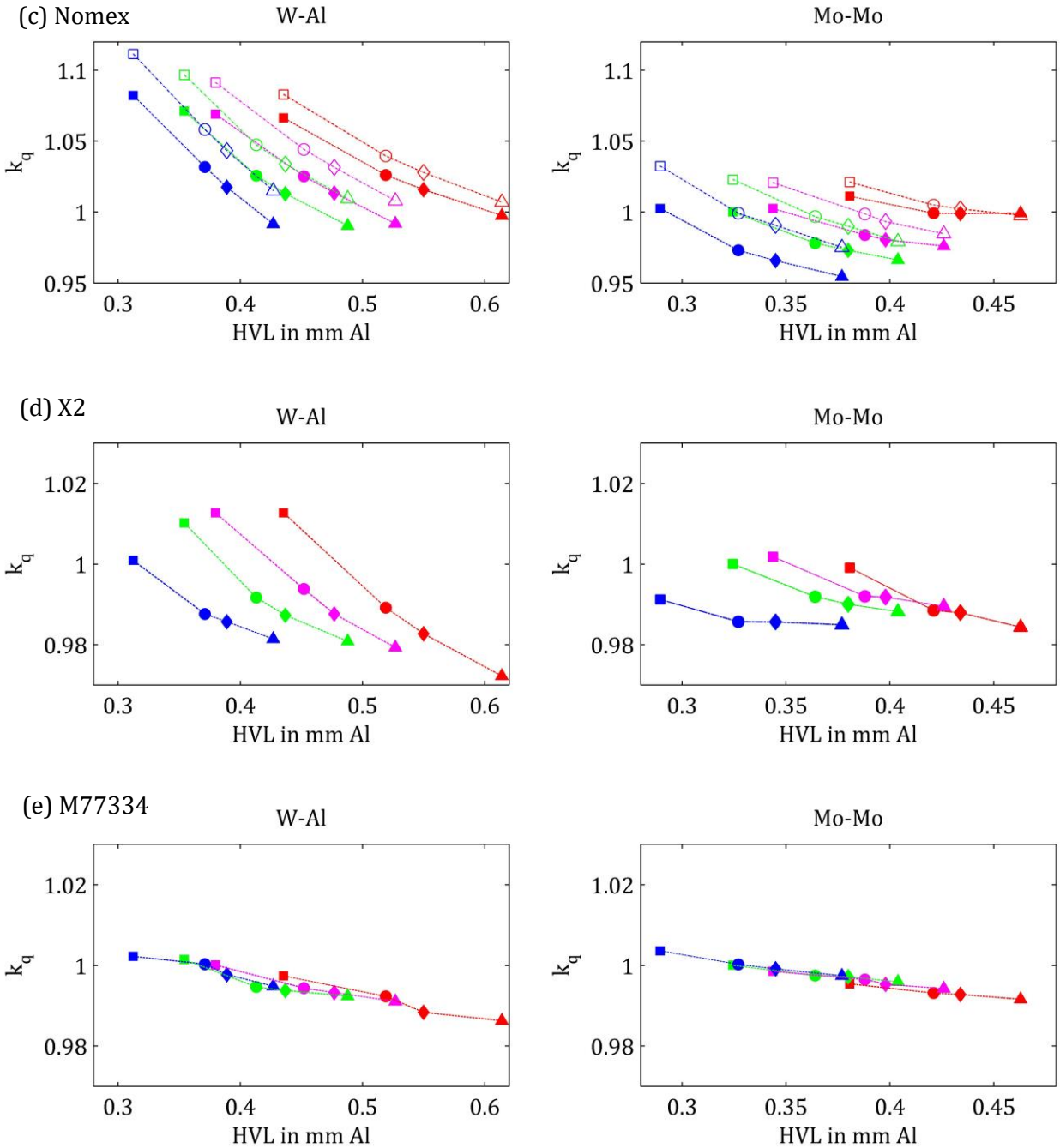

Figure 4.3 (a) to (e): square: 0 *mm* PMMA; circle: 1.986 *mm* PMMA; diamond: 2.775 *mm* PMMA triangle: 4.761 *mm* PMMA; blue: 25 *kV*; green: 28 *kV*; magenta: 30 *kV*; red: 35 *kV,*
Closed markers: "no compression paddle"; open markers: "compression paddle"
The scale for the k_q axis is adapted to the individual variation of the dosimeters. The open and Closed markers in (d) left are overlapping.

4.3
Grouping of dosimeters

To investigate the built-in correction of the dosimeters tested calibration points for radiation qualities different from the selection in the software were determined. According to their maximum of variation the dosimeters were classified in three groups. The maximum of variation M is the maximum value of

$$M = \begin{cases} |1 - \min(\mathrm{R})| \\ |1 - \max(R)| \end{cases} . \qquad (4.1)$$

R is the response $1/k_q$, 1/(HVL ratio) and 1/(kVp ratio), respectively. The range of variation for all dosimeters tested is listed in Table 4.3. The dosimeters in group 1 failed the limits of variation of ±5% for air kerma rate measurement stated by the manufacturers and recommended by the international standard IEC 61674 [1]. The dosimeters in group 2 meet the recommended limits for the calibration with appropriate selected radiation quality but failed for at least one inappropriate selection of the radiation quality in the software. The dosimeters in group 3 remain into the limits even if the selected radiation quality in the software is wrong. Due to the low energy dependence of its response the tested ionization chamber is in group 3 although there is no built-in correction. The uncertainty for Nomex is stated by the manufacturer with ±2.5%, this is fulfilled by the dosimeter.

Table 4.3: Range of variation for appropriate selection of the radiation quality in the software (correct selection) and for wrong selected radiation qualities (wrong selection).

	Measuring Assembly	**Max deviation from 1 in %**	
		correct selection	**wrong selection**
Group 1	Piranha 657	-10 to +13	-18 to +38
	Barracuda, R100B	-6 to +9	-6 to +31
	Mult-O-Meter	-12 to -5	-12 to +18
Group 2	Black Piranha	-3 to +1	-16 to +19
	Nomex	-1 to +1	-23 to +4
	Xi	-3 to +1	-18 to +2
Group 3	Accu Gold, AGMS-DM+	0 to +2	-3 to +2
	X2	-2 to 2	-2 to +2
	M77334	-1 to 1	–

4.4
Built-in correction

Figure 4.4 shows the correction factors k_q as a function of HVL for the dosimeters in group 1. Barracuda with R100B and Mult-O-Meter (subfigure (a) and (b)) do not apply an internal correction of the energy dependence of their response. The open circles represent calibration points determined with other radiation qualities than Mo-Mo. The result of the Piranha 657 is shown in Figure 4.4 (c). Markers represent the k_q values for appropriate selection of the radiation quality in the software. The vertical lines represent the range of k_q for radiation qualities deviating from the selected one. The 5% limit is represented by red horizontal lines. The results for dosimeters in group 2 and 3 are shown in Figure 4.5 and Figure 4.6, respectively.

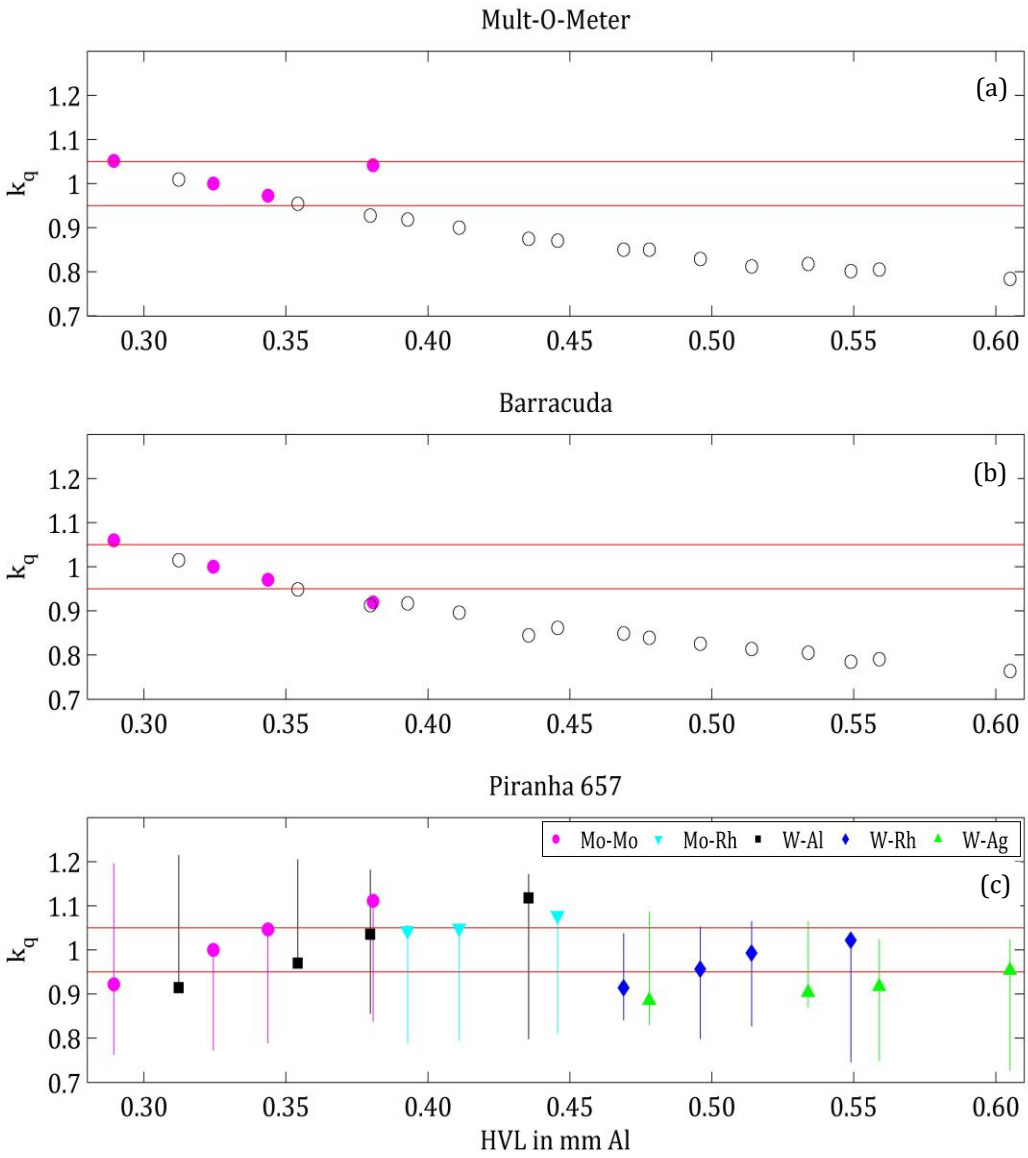

Figure 4.4: Dosimeters of group 1. Closed markers: correction factors k_q to the standard radiation quality Mo-Mo 28 for calibration with appropriate selected radiation quality. Open circles in (a) and (b): k_q determined with other radiation qualities than selected. Vertical lines in (c): range of k_q for the wrong selection. The red horizontal lines are ±5%.

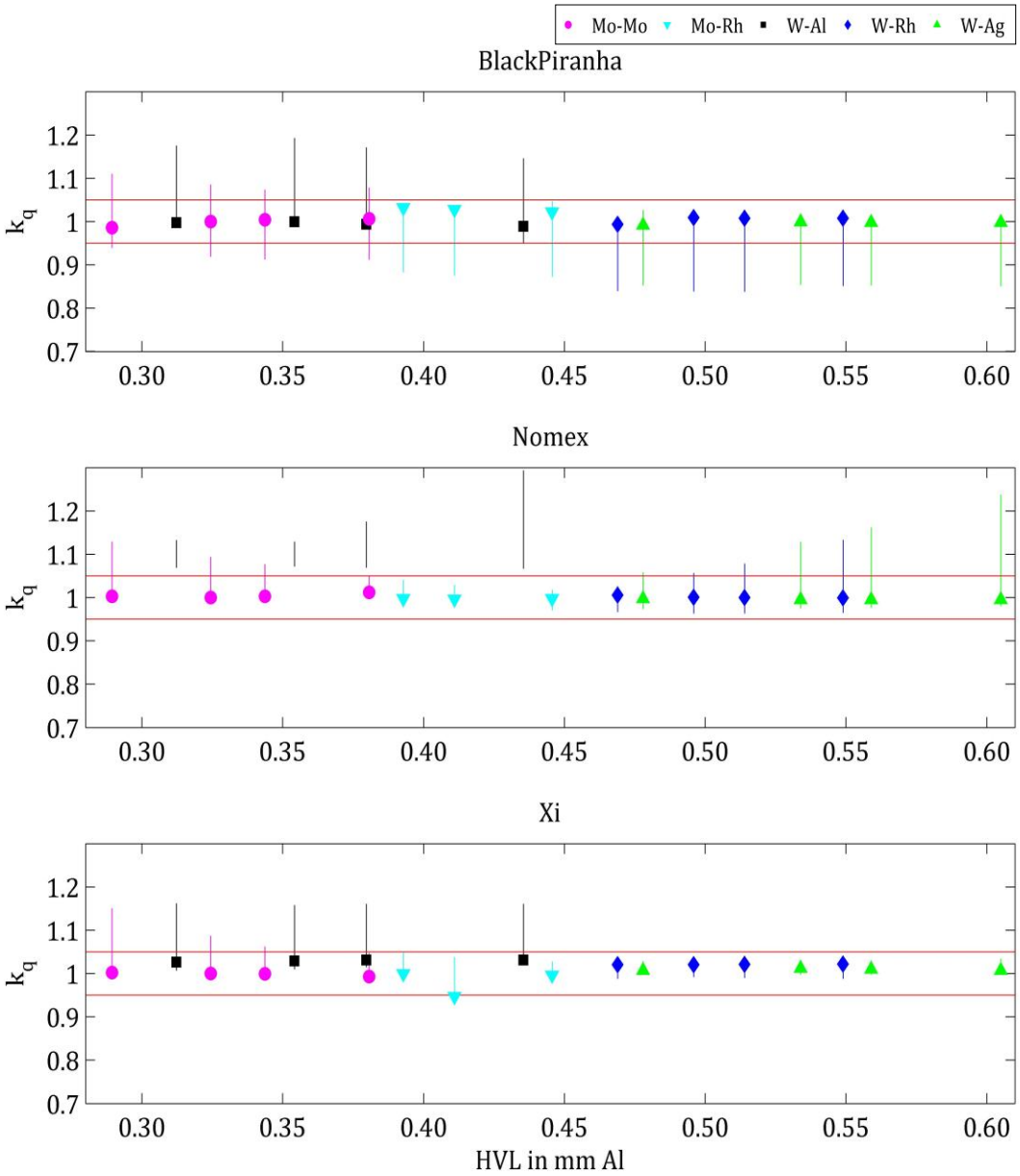

Figure 4.5: Data for dosimeters in group 2 presented accordingly to Figure 4.4 (c).

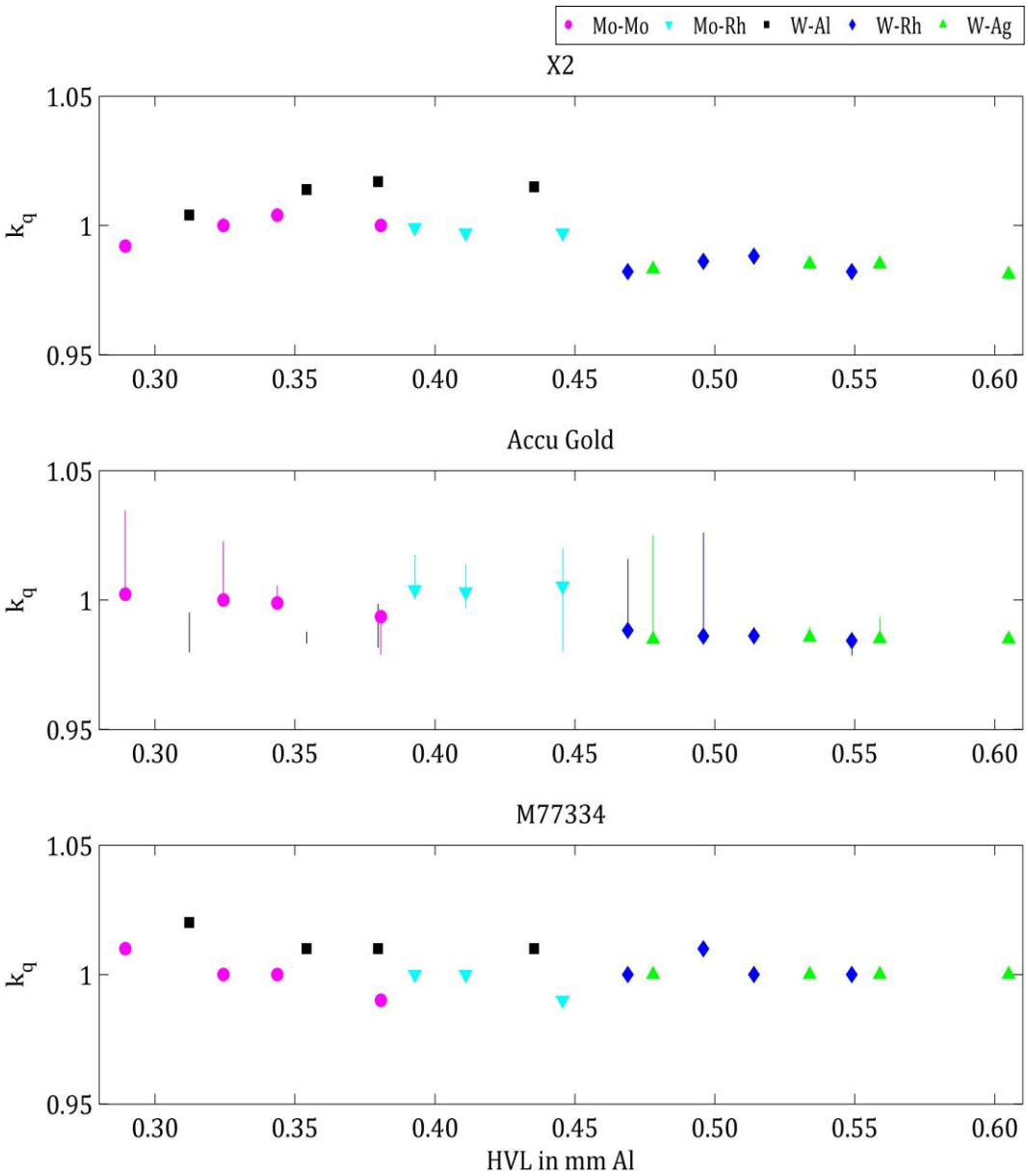

Figure 4.6: Data for dosimeters of group 3 presented accordingly to Figure 4.4 (c). The range of the k_q axis is adapted to the smaller variation of the dosimeters of group 3.

4.5
Calibration factors for half-value layer measurement

Five of the dosimeters tested were capable of measuring HVL. The maximum error in short term repeatability was ±0.007 *mm* Al. Accu Gold did not measure HVL for W-Ag 35. The accuracy of the HVL measurement was stated by every manufacturer in a different way. Just two dosimeters fulfill their own limits. Table 4.4. shows the HVL ratio as a function of radiation quality for each dosimeter tested. The detailed data are listed in the Appendix.

Table 4.4: Accuracy of HVL measurements. M is determined according equation (4.2).

	Measuring assembly	Limit in the manual	Max deviation M	Range of 1/HVL ratio	
				correct selection	wrong selection
fail	Black Piranha	±10%	11%	-3 to +11	-31 to +48
	Nomex	±0.01 *mm* Al	0.04 *mm* Al	-4 to +7	-17 to + 62
	Xi	±5%	11%	+1 to +11	-13 to +36
pass	Accu Gold	±10%	7%	-7 to +1	-7 to +14
	X2	±5%	4%	-4 to +3	-4 to +3

4.6
Calibration factors for tube voltage measurements

Six of the dosimeters tested were capable of measuring tube voltage. The maximum standard deviation for determining short term repeatability is ±0.1 *kVp*. Based on the manual Xi and X2 require additional 0.5 *mm* Al filtration for *kVp* measurements of Mo-Rh. X2 did not provide a result for Mo-Rh. Without additional filtration of 0.5 *mm* Al the air kerma rate at the point of test is 0.83 *mGy/s*. The additional filtration reduces the air kerma rate to approximately 0.06 *mGy/s*. With increased air kerma rate (approximately above 0.1 *mGy/s*), measurement results for Mo-Rh 30 and Mo-Rh 35 could be obtained but not for Mo-Rh 28. Xi did not measure *kVp* for the radiation quality W-Ag. Detailed data are listed in the appendix.

Table 4.5: Accuracy of kVp measurements. L is determined according to (4.2).

	Measuring assembly	Limit in the manual	Max deviation M	Range of 1/kVp ratio	
				correct selection	wrong selection
fail	Piranha 657	±2%	13%	-10 to +13	-18 to +38
	Black Piranha	±2%	10%	+1 to + 10	-30 to + 68
	Nomex	±0.5 *kV*	2.4 *kV*	-2 to +8	-30 to +52
	Xi	±2%	7%	0 to +7	-30 to +41
	Accu Gold	±2%	9%	-9 to +8	-31 to + 75
	X2	±2%	6%	-6 to -1	-30 to +47

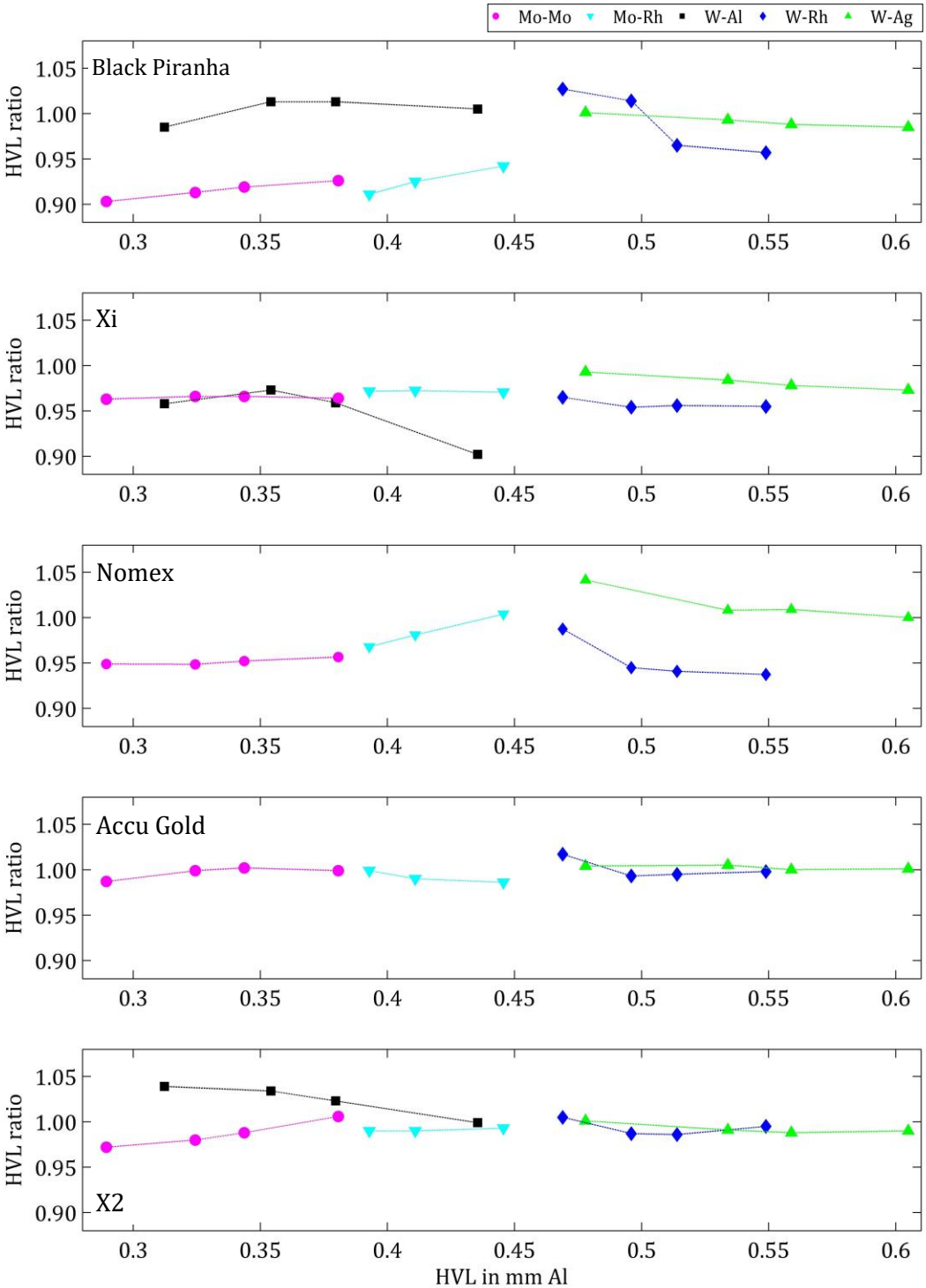

Figure 4.7: Calibration factor for HVL measurements. Ratio of HVL and measured HVL as a function of reference HVL.

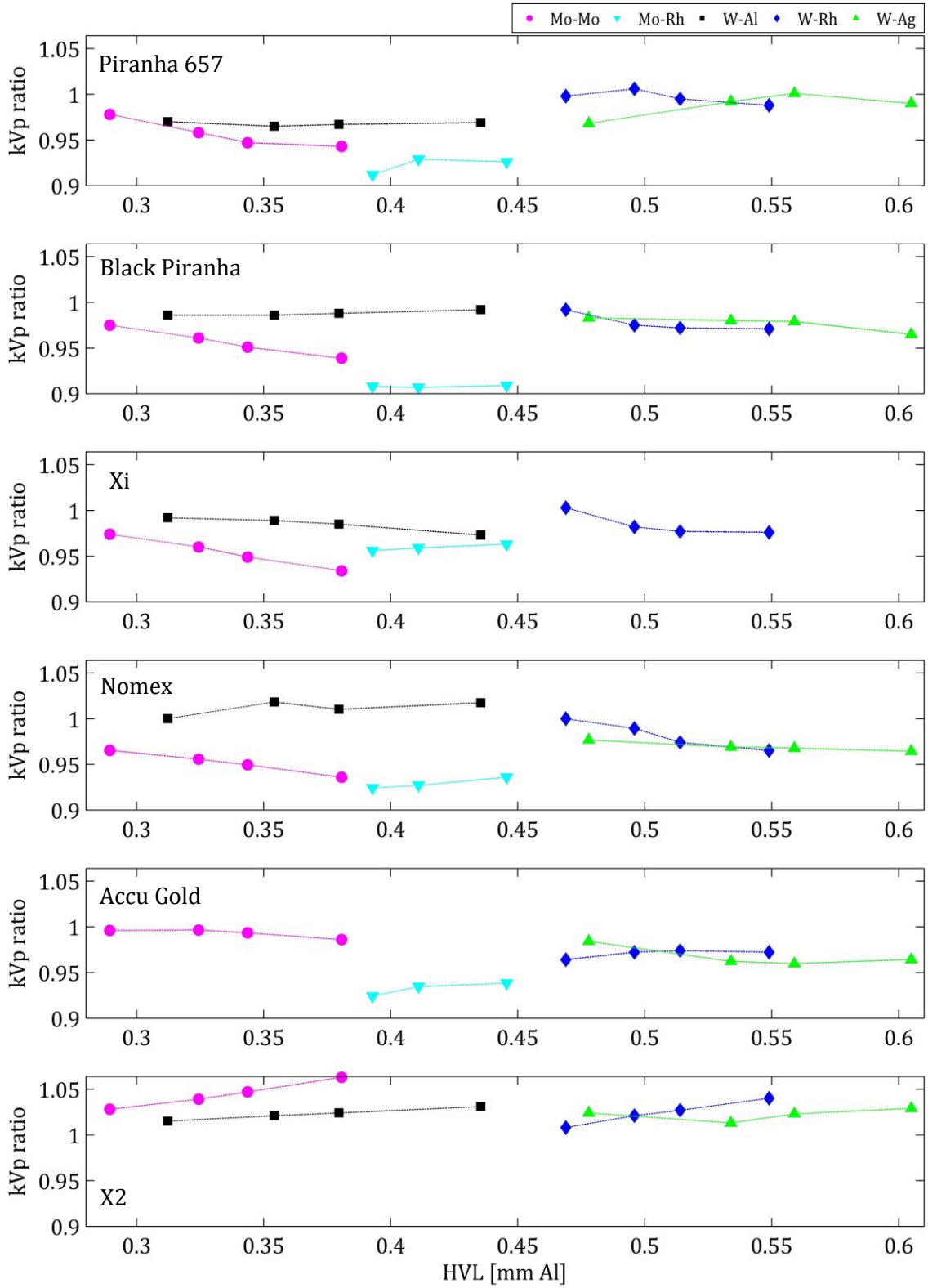

Figure 4.8: Calibration factor for *kVp* measurements. Ratio of *kVp* and measured *kVp* as a function of reference HVL.

4.7
Uncertainties

Measurement uncertainties were estimated according to [37] and [38]. Based on their method on estimation the uncertainties are classified as type A or type B. Type A uncertainties are evaluated with statistical methods. Type B uncertainties are determined by other means.

The contributions to the total relative uncertainty in the calibration factor are evaluated in two steps. The first one corresponds to uncertainties arising from pinpointing the reference air kerma rate with the reference standard or working standard. The other one relates to the uncertainties linked to the dosimeter to be calibrated. The used reference standard for this study was a working standard of the IAEA dosimetry laboratory (DOL) and was calibrated against the DOL`s reference standard (see section 3.3). The estimated relative uncertainty for this calibration is given in Table 4.7. The model equation for uncertainty estimation of the calibration factors *N* for the user dosimeters is

$$N = \frac{\dot{K}_{air}}{\dot{M}_{air}} \frac{k_{stability} k_Q k_{pos} k_{elec} k_{TP} k_{monitor}}{k_{pos} k_{read}} \quad . \tag{4.2}$$

$\dot{K}_{air}$ corresponds to the reference air kerma rate, $\dot{M}_{air}$ to the air kerma rate reading of the user dosimeter. The applicable correction factors are listed in Table 4.6. $k_{stability}$ considers the effect of the stability of the instrument (ionization chamber and electrometer), the correction for change in a source position, the available calibration coefficients of the reference standard chambers and a change in the X-ray tube output rate which is estimated from a series of output rate measurements. It is dominated by a component having an evaluation of Type A and has an effective number of degrees of freedom of about 50. It is treated as Type B because this component is not directly determined during each measurement.

The relative combined standard uncertainty for the user dosimeters is given in Table 4.8. The type B uncertainties for the current, temperature and pressure measurement are stated in their calibration certificates. The type A uncertainty of the electrometer includes the statistics for temperature and pressure measurement. The monitor chamber contribution is the maximum coefficient of variation c_v for the monitor chamber readings of the individual measurements. In equation (4.3) σ_a represent the standard deviation of the individual measurements, a_{ave} represent the average of the individual measurements.

$$c_v = \frac{\sigma_a}{a_{ave}} \tag{4.3}$$

According to equation (4.2) two correction factors correspond to the uncertainty linked to the user dosimeter. For determining the contribution of the positioning propagation of error and the inverse square law are employed. The propagation of error is the effect of variables` uncertainties on the uncertainty of a function based on them. It is calculated according equation (4.4) where s_f represents the absolute standard uncertainty of the function *f*, $\sigma_x$represents the standard deviation of *x* and so forth. To determine the standard deviation of *x* the half of the interval of all possible values is divided to the standard uncertainty of the distribution (see Figure 4.9). The uncertainty in positioning appears in terms of deviating intensity which is proportional to the invers square of the distance. A maximum error in positioning of 0.2 *mm* and a rectangular distribution are assumed. To obtain the relative standard uncertainty the absolute standard uncertainty s (see equation (4.7)) is divided by the quantity *I(r)* (see equation (4.5)). The second uncertainty related to the measurement with the user dosimeter is the maximum coefficient of variation c_v (see equation (4.3)) of the individual measurements.

$$s_f = \sqrt{\left(\frac{\partial f}{\partial x}\right)^2 \sigma_x^2 + \left(\frac{\partial f}{\partial y}\right)^2 \sigma_y^2 + \cdots} \tag{4.4}$$

$$s = \sqrt{\left(\frac{dI(r)}{dr}\right)^2 (\sigma_r)^2} \tag{4.7}$$

$$I(r) = \frac{const.}{r^2} \tag{4.5}$$

$$\sigma_r = \frac{a}{\sqrt{3}} \tag{4.6}$$

Table 4.6: Correction factors for the model equation.

Correction factor	**Explanation**
$k_{stability}$	Correction for the effect of a change of the DOL secondary standard dosimetry system.
k_Q	Correction for any change in the beam quality from the PSDL
k_{pos}	Correction for the deviation of chamber or dosimeter position from the reference point.
k_{elec}	Calibration coefficient of the electrometer.
k_{TP}	Correction for temperature and pressure.
$k_{monitor}$	Ratio of the monitor chamber reading simultaneously with the reference chamber and the dosimeter to be calibrated, respectively.
k_{read}	Coefficient of variation of the individual dosimeter readings.

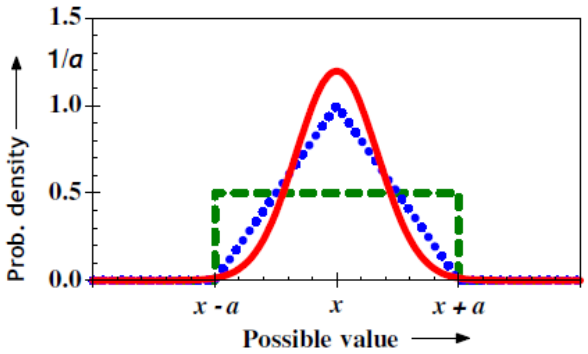

Distribution	**Standard uncertainty**
rectangular	$\frac{a}{\sqrt{3}}$
triangular	$\frac{a}{\sqrt{6}}$
Gaussian	$\frac{a}{3}$

Figure 4.9: Probability density distribution. Red: Gaussian, blue, triangular, green: rectangular

Table 4.7: Estimated relative standard uncertainty (%) for the calibration factor *N*.

Calibration of the working standard	**Type A**	**Type B**
Step 1: DOL reference standard		
Calibration from BIPM/PSDL		0.48
Long term stability of the reference standard		0.30
Spectral difference of the beam at DOL and PSDL		0.10
Chamber positioning		0.03
Current measurements including range and time- based corrections of IAEA electrometer	0.02	0.05
Uncertainty due to temperature measurements		0.03
Uncertainty due to pressure measurements		0.01
Monitor chamber contribution	0.02	
Relative combined standard uncertainty of $\dot{K}_{air}$ (Step 1)	0.03	0.58
Step 2: Instrument to be calibrated (working standard)		
Chamber positioning		0.03
Current measurements including range and time- based corrections of IAEA electrometer	0.02	0.05
Uncertainty due to temperature measurements	0.01	0.03
Uncertainty due to pressure measurements	0.01	0.01
Monitor chamber contribution	0.02	
Difference in radial non- uniformity of the beam		0.25
Relative combined standard uncertainty Step 2	0.03	0.26
Relative combined standard uncertainty Step 1+2	0.04	0.63
Relative expanded uncertainty (k=2) working standard		**1.27**

Table 4.8: estimated relative uncertainty (%) for the user dosimeters.

Calibration of the user dosimeter	**Type A**	**Type B**
Step 1: Working standard		
Chamber positioning		0.03
Current measurements including range and time- based corrections of IAEA electrometer	0.02	0.05
Uncertainty due to temperature measurements	0.01	0.03
Uncertainty due to pressure measurements	0.01	0.01
Monitor chamber contribution	0.02	
Relative combined standard uncertainty of $\dot{K}_{air}$ (Step 1)	0.03	0.07

Continuation of Table 4.8.

Step 2: User dosimeter		
Positioning		0.03
Reading (Piranha 657)	0.10	
Relative combined standard uncertainty Step 2	0.10	0.03
Relative expanded uncertainty (k=2) Step 2		0.25
Relative expanded uncertainty (k=2) for N (Red Piranha)		**1.30**
Reading (Barracuda, R100B)	0.03	
Relative combined standard uncertainty Step 2	0.03	0.03
Relative expanded uncertainty (k=2)		0.16
Relative expanded uncertainty (k=2) for N (Barracuda)		**1.28**
Reading (Mult-O-Meter)	0.03	
Relative combined standard uncertainty Step 2	0.45	0.03
Relative expanded uncertainty (k=2)		0.91
Relative expanded uncertainty (k=2) for N (Mult-O-Meter)		**1.56**
Reading (Black Piranha)	0.10	
Relative combined standard uncertainty Step 2	0.10	0.03
Relative expanded uncertainty (k=2)		0.25
Relative expanded uncertainty (k=2) for N (Black Piranha)		**1.30**
Reading (Nomex)	0	
Relative combined standard uncertainty Step 2	0	0.03
Relative expanded uncertainty (k=2)		0.16
Relative expanded uncertainty (k=2) for N (Nomex)		**1.28**
Reading (Xi)	1.70	
Relative combined standard uncertainty Step 2	0.20	0.03
Relative expanded uncertainty (k=2)		0.43
Relative expanded uncertainty (k=2) for N (Xi)		**1.34**
Reading (Accu Gold, AGMS-DM+)	0.08	
Relative combined standard uncertainty Step 2	0.08	0.03
Relative expanded uncertainty (k=2)		0.22
Relative expanded uncertainty (k=2) for N (Accu Gold, AGMS-DM+)		**1.29**
Reading (X2)	0.20	
Relative combined standard uncertainty Step 2	0.20	0.03
Relative expanded uncertainty (k=2)		0.43
Relative expanded uncertainty (k=2) for N (X2)		**1.34**

5 Discussion

Measurement of air kerma rate

The number of semiconductor dosimeters employed for quality control and general dosimetry in clinical practice of X-ray imaging is increasing. Modern mammography units use a variety of radiation qualities but for calibration purpose the international standard IEC 61267 [1] only considers one set of radiation qualities based on the anode-filter combination Mo-Mo. The effect of the radiation quality on the calibration factor of eight semiconductor dosimeters and one ionization chamber was studied. The results indicate the need of complementing the international standard IEC 61267 [1] to cover different clinical radiation qualities for calibration and provide guidance for the calibration of semiconductor dosimeters.

Large differences between the dosimeters were found. An error up to 16% can occur if no calibration factor is applied. If only the calibration factor for the standard radiation quality Mo-Mo 28 is applied for measurement with different radiation qualities, the error reduces to maximum 13%. As recommended by the international standard IEC 61674 [2], the limits of variation for all semiconductor dosimeters tested was stated in their manual with ±5% and for Nomex it was even lower (±2.5%). All except three dosimeters fulfilled their own specification of accuracy for air kerma rate measurements.

Impact of beam hardening by PMMA

The impact of beam hardening caused by additional filtration of a compression paddle e.g. on the calibration factor for four semiconductor dosimeters and one ionization chamber was investigated. Two different anode-filter combinations (W-Al, Mo-Mo) and PMMA sheets of 3 different thicknesses were used. Barracuda with R100B dose probe represented a dosimeter without compensation of the energy dependence of the response in the software, Black Piranha, Nomex representing meters of group 2 and X2 representing a meter of group 3 dosimeters with internal compensation. Black Piranha, Nomex and X2 were tested in two different modes: “no compression paddle” and “compression paddle” selected in the software. For Black Piranha and Nomex the selection of the use of a compression paddle in the software affects the reading applying an additional internal correction. This factor is in the range of 1.02 and 1.07 for Black Piranha and between 1.00 and 1.03 for Nomex for 1.9 mm to 4.7 mm PMMA. The k_q values without internal compensation for the compression paddle selected was from 0.88 to 1.01 and 0.95 to 1.08 for Black Piranha and Nomex, respectively. Applying the internal correction for the compression paddle k_q is increased from 0.93 to 1.04 and 0.98 to 1.11 for Black Piranha and Nomex, respectively.

X2 does not have the option to select the use of a compression paddle for W-Al. Other than for W-Al the option to select a compression paddle is available for other anode-filter combinations as Mo-Mo. For Mo-Mo it was tested in both modes, but the selection does not affect the reading of dose rate. Even if the correct calibration factor for the used anode-filter combination is applied the maximum error occurs with additional PMMA in the beam can be up to 11%. The ionization chamber tested showed the least energy dependence of the response. Its occurring error with additional PMMA was 0.9%. One shortage of this study was that no clinically used compression paddles were available and PMMA may not fully represent their composition.

Built-in compensation of the energy dependence of the response

To correct for their energy dependence of the response most of the semiconductor dosimeters tested require a pre-selection of the radiation quality in the software. Calibration factors for five different anode-filter combinations were determined for the appropriate selection as well as for deviant selection. However, inappropriate settings of the radiation quality in the system menu of the dosimeter where typically not identified by the meter resulting in erroneous readings. The

performance of the individual dosimeters showed a large variation. Only Accu Gold displayed error messages for dose rate measurement for W-anode if a Mo-anode is selected in the software. All other dosimeters provided readings for every combination. The largest range of calibration factors for appropriate selected radiation quality showed Piranha 657 (-10% to +13%). For inappropriate selection of the radiation quality in the software the range increased up to -23% (Nomex) and +38% (Piranha 657).

As described in section 4.3 the dosimeters were divided into 3 groups. Dosimeters of group 1 failed the 5% limit even for the correct use. Dosimeters of group 2 fulfill this limit for appropriate selection of the radiation quality in the software but exceeded it for wrong selection. Nomex is the only dosimeter which stated a 2.5% limit in the manual. For appropriate selection the maximum variation was 1% but up to 23% for wrong selection. Dosimeters which stay within the 5% limit even for wrong selection in the software are in group 3. The range of calibration factors for the correct use was maximum 21% for dosimeters of group 1 (Piranha 657 for W-Ag 25) and 4% for dosimeters of group 2 and 3 (Black Piranha, Xi and X2). The ionization chamber tested had the least energy dependent response with 1.7%. The biggest range of calibration factors appeared for Mo-Mo 35 (minimum value 0.86 for Barracuda with R100B, maximum value 1.18 for Piranha 657).

For all three dosimeters of group 2 the largest error in the reading of dose rate for other radiation qualities as selected in the meter menu occurs for W-Al. Even if for some radiation qualities and different selections the calibration factor remains within the specified accuracy limits of 5% all dosimeters of group 2 exceeded the limit for measuring W-Al. For Xi the selection of W-Ag for W-Al 25 results in an error of +16%. For Black Piranha the selection of W-Rh for W-Al 28 results in an error of +20%. For Nomex the selection of Mo-Mo for W-Al 35 results in an error of +31%. For dosimeters of group 3 the calibration factor is nearly independent of the radiation quality and stays within the 5% limits for any selection in the software. By calibrating dosimeters with different selections in the software with only the anode-filter combination W-Al, and a tube voltage range from 25 to 35 *kV*, it is possible to classify a user dosimeter into either group 1, 2, or 3.

Some dosimeters have the tendency to indicate too low or to high dose rate readings dependent on the anode-filter combination. Black Piranha provided too high readings of dose rate for W-Al for all radiation qualities selected in the software except the correct one. Nomex shows dependency on the anode material. For qualities with W-anode the biggest deviation of the calibration factor arises from the selection of Mo-Mo. For the radiation quality Mo-Mo the selection of W-Al caused the biggest variation. The internal compensation method for Xi works properly for higher HVL of the radiation qualities used. For the anode- filter combinations W-Rh and W-Ag the readings of dose rate remain within the 5% accuracy limit independent of the selected radiation quality in the software. If Mo-Rh or Mo-Mo is selected Xi remains within the 5% limit independent of the used radiation quality. Nomex is the only dosimeter which provided a too low dose rate for all radiation qualities. The readings of Xi and X2 were too low or too high for all tube voltages of an anode-filter combination. Xi provided too low readings for all qualities with W-anode and too high readings for all qualities with Mo-anode. X2 provided too high readings for W-Rh and W-Ag and too low for all other radiation qualities. All other dosimeters have at least one radiation quality where the calibration factor is below and larger than one for different tube voltages of an anode-filter combination.Based on these results, the build-in correction is operating well for dosimeters in groups 2 and 3. The dosimeters in group 3 are independent of the pre-selection of the radiation quality and they correct properly based on the measured data. Most of the semiconductor dosimeters tested are operated by individual dosimetry software provided by the manufacturer. The software should be updated regularly. However, it is possible that a software update changes the inherent calibration factors and it should be kept in mind that this change may not necessarily be recognized by the user.

Measurement of HVL

Xi and X2 provided HVL readings for every anode-filter combination and radiation quality selected in the software. Black Piranha failed for the selection of Mo-Rh and Mo-Mo for the radiation quality W-Al 35 and W-Ag 35, respectively. Accu Gold and Nomex did not measure for

most qualities with W-anode with the selection of a Mo-anode. Individual results for each dosimeter are listed in the appendix. All dosimeters of group 2 did not meet the specifications of the manufacturer for HVL measurements for appropriate selection of the radiation quality. Both dosimeters of group 3 fulfill their own accuracy limits. The accuracy of HVL measurements and the accuracy of dose and dose rate measurement seem to be dependent. While for dosimeters of group 2 the difference of HVL ratio and calibration factor *N* can be up to 12%, the difference for dosimeters of group 3 is much smaller (up to 3%). Inaccurate measuring results of HVL have an impact on the calculation of the mean glandular dose. The correction factors which required to convert the incident air kerma to MGD are tabulated as a function of HVL in [5]–[7]. There, HVL is given with three digits where the last digit can be either zero or 5. Thus, due to the error induced by rounding small deviations of the measured from the true value can have big impact. For example, the product of the tabulated correction factors *g* and *c* (see equation (2.3)) for a breast of 5 cm thickness differ up to 10% for a given HVL of 0.40 and 0.45 mm Al, respectively.

Measurement of *kVp*

The maximal error for tube voltage measurements was +10% for dosimeters of group 1 and 2 and +8% for dosimeters in group 3. Thus, no dosimeters fulfill the manufacturer specifications although the short-term reproducibility was maximum 0.3%. Xi failed for measuring *kVp* for W-Ag and X2 for Mo-Rh. It is assumed, that the low air kerma rate on the SSDL system causes this malfunction. The measurements were repeated with higher dose rates and X2 measured tube voltage for Mo-Rh 30 and 35 for dose rates higher than 0.1 *mGy/s* (reading of X2) but not for Mo-Rh 28. Brateman and Heintz [22] studied the performance of five semiconductor dosimeters on two clinical mammography units. Four of them were also tested in the present study (Piranha 657, Nomex, Xi and Accu Gold). The Accu Gold was tested by Brateman and Heintz with the external probe AGMS-M but in this study the external probe AGMS-DM+ was used. For qualities with W-anode the results for *kVp* measurements are comparable but for qualities with Mo-anode the deviation in the present study is much higher. The absolute values of differences from the *kVp* set in the study of Brateman and Heintz was maximum 1.1 *kV* measured by Xi for Mo-Rh but 1.3 to 2.6 *kV* for qualities with Mo-anode in the present study. There was one exception, the absolute value of the differences from the *kVp* set for the Mo-Mo measured by Accu Gold was much lower than for all other dosimeters tested (0.2 *kVp*). In the study of Bratemen and Heintz the Xi also failed to measure *kVp* for W-Ag.For the dosimeters tested the accuracy in *kVp* measurement was more accurate on clinical mammography units. Thus, the performance depends on if the meter is used with an SSDL system or with a clinical unit. This indicates that this measurement capability is optimized for clinical use. The accuracy of absolute *kVp* measurements with semiconductor dosimeters is not so high but maybe they could be used for relative measurements and for regular quality control. However, in this case the long-term reproducibility should be studied more.

Issued occurred during measurements

During large sets of measurements in 2017 we found suspicious results. The sets where these results occurred were repeated and the reasons were found. Some strange behavior in one set of measurements with one of the meters (Xi) was repeated but no explanation was found. There was a clear difference of the calibration factor and HVL ratio for Mo-Rh 30 to the values for all other radiation qualities. To obtain these values the Mo-anode with Rh filter and 30 kV tube voltage was employed. The X-ray beam was continuously on and just the shutter was opened and closed to start and stop the readings. The only variable during this set of measurements was the selection of the radiation quality in the software. First, 3 readings each 10 *s* with the reference ionization chamber were taken, then 3 readings each 10 *s* with Xi followed by 3 readings with the reference chamber. After this sequence the radiation quality in the software was changed. First, W-Al was selected followed by W-Rh, W-Ag, Mo-Rh and Mo-Mo. All results achieved before and after the selection of Mo-Rh remained within the accuracy limits specified by the manufacturer. For Mo-Rh 30 and appropriate selection of the radiation quality in the software the determined calibration factor was 0.944 and the HVL ratio was 1.162. The

maximum variation was -6% and +16%, respectively. The coefficients of variation for these individual measurements were 1.7% for dose rate and 1.9% for HVL. For inappropriate selection in the software the calibration factors were between 0.993 (selection Mo-Mo) and 1.034 (selection W-Rh). The HVL ratio for inappropriate selection was between 0.961 (selection W-Rh) and 0.994 (selection W-Ag). It is remarkable that the results for appropriate selection of the radiation quality in the software exceed the accuracy limits specified by the manufacturer. For the readings with other radiation qualities the coefficient of variation was maximum 0.2% for dose rate and HVL measurements. The monitor chamber was not read simultaneously but less than a minute before and after Xi. Since the coefficient of variation of the monitor chamber readings was less than 0.01% one can assume that the tube output was stable during the entire time span of the measurements. This abnormality was the reason for the repetition of the measurements with Mo-anode for all different selections in the software. To verify the repeatability the measurements with W-anode and appropriate selected radiation quality in the software were also repeated.

The measurement protocol and set-up for the repetition were the same as for the original set of measurements. The calibration factors for radiation qualities with W-anode for the original and repeated measurements remain within 1%. The difference between the original and the repeated measurements for Mo-Rh 28 and Mo-Rh 35 and appropriate selection in the software was less than 0.5%. For the suspicious value of the original measurements the difference was 5% and 20% for dose rate and HVL measurements, respectively. For inappropriate selection in the software the repeated measurements deviate up to 1.6% (Mo-Rh with selection W-Ag) from the originals. For Mo-Mo and correct selection in the software the difference between the original and repeated measurement of dose rate was less than 1% but an abnormality occurs for the selection of W-Al. There the difference was 2.9% for dose rate and 25% for HVL measurement. The coefficient of variation for these individual measurements was 0.04% and 0.1%, respectively. The uncertainty of the calibration factor for Xi is 1.28%. For this study the results of the original set of measurements were used. Only the set of measurements for Mo-Rh and appropriate selection in the software were substituted by the results of the repeated measurements. It is assumed that Xi use different internal compensation modes to correct for the energy dependence of the response. How the software of Xi select the applied correction is incomprehensible. However, experimental issues with these meters occurring at SSDL settings might not be evident in clinical measurements.

The manufacturer was contacted to provide explanation. They replied that all their instruments are verified on any mammography machines on the market. If the behavior of an X-ray machine or the measurement set-up differs from what is the normal spectrum for the intended use it is difficult to say how the instrument can be expected to behave. They tried to repeat the measurements but where not even able to simulate the measurement conditions of the IAEA DOL in their laboratory. For the manufacturer, there are some unknown factors which cannot be verified when it comes to the described behavior of the Xi MAM sensor. Differences between clinical mammography units and the set-up in a calibration laboratory as anode angle, distance to the focal spot, tube current and short exposure time as possible reasons.

This issue shows that unpredictable behavior of semiconductor dosimeters can cause large errors in the measurement results. For measurements performed on clinical mammography units it can be challenging to reveal this kind of errors in operation. In calibration laboratories the use of reference level instruments allows for easier detection of these issues. Anyway, each dosimetry equipment will need a calibration and it should be possible to perform this in a calibration laboratory. Even though there are some differences between the X-ray systems used in clinical and calibration practice, it should be possible to do representative calibrations. The possibility to modify the calibration set-up to simulate the clinical beam more closely should be taken into account. Normally, the dose rate or anode angle of an existing tube cannot be changed. However, it would be possible to select radiation qualities which are closer to the clinical practice.

6 Conclusion

The performance of eight semiconductor dosimeters with five different radiation qualities and different measuring modes was tested under calibration conditions. In IEC 61267 [1] just one set of radiation qualities based on the anode-filter combination Mo-Mo is defined as standard radiation conditions for calibration of mammography dosimeters. IEC 61674 [2] defines limits of variation for the energy dependence of response for mammography dosimeters with ±5% for 25-35 kV. However, the standard acknowledges that other ranges for different anode-filter combinations are possible. Nevertheless, for other anode-filter combinations than Mo-Mo no limits or guidance are provided.

As found by previous studies the energy dependence of the response is more pronounced than for ionization chambers. In addition, the energy dependence of the response is different for each dosimeter and not predictable. Thus, calibration with just one radiation quality cannot be recommended. If possible, the dosimeters should be calibrated for all radiation qualities for which it is intended to be used. However, the differences between the X-ray facility in the SSDL and the clinical mammography unit as anode angle, dose rate and ripple cannot be neglected. To investigate the difference of the performance of semiconductor dosimeters on an SSDL X-ray calibration set-up and on a clinical mammography unit further studies are required. It should be kept in mind that it is necessary to be able to test measuring instruments under reference conditions.

No dosimeter tested fulfilled the accuracy limits stated by the manufacturer for *kVp* measurement. Only two dosimeters (Accu Gold, X2) fulfilled the limits for HVL measurements. These limitations support the assumption that the performance of the HVL and tube voltage measurement of semiconductor dosimeters is optimized for the quality control purpose and repeated relative measurements with a fixed radiation quality which is typically used with clinical mammography units.

A
Appendix

A.1
Dosimeters calibrated

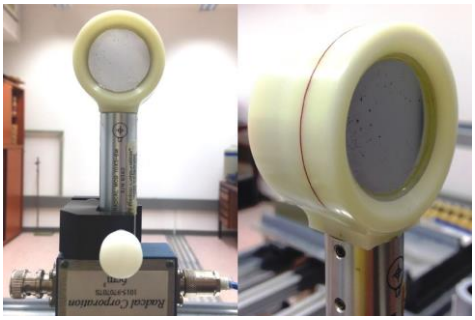

Figure A.1: Reference standard

Figure A.2: left: Piranha 657, right: Black Piranha

Figure A.3: Barracuda with dose probe R100B

Figure A.4: Mult-O-Meter

Figure A.5: Accu Gold with dose probe AGMS- DM+

Figure A.6: Xi with MAM sensor

Figure A.7: Nomex

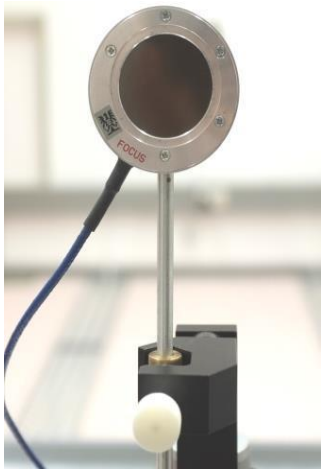

Figure A.8: M77334

Figure A.9: MAM dose probe of X2

A.2
Calibration factors

Tables A.1. to A.13. show the calibration factors *N*, HVL ratio and *kVp* ratio for all dosimeters tested for different selections of the radiation quality in the software. The values in bold indicate the appropriate selection of the radiation quality.

Table A.1: Calibration factors for Barracuda, Mult-O-Meter and ionization chamber M77334.

Calibration factor *N*			
Applied radiation quality	**Barracuda**	**Mult-O-Meter**	**M 77334**
	Calibration		
	Mo-Mo	**Mo-Mo**	**Nk in mGy/nC**
W-Al 25	0.953	1.023	24.271
W-Al 28	0.891	0.967	24.252
W-Al 30	0.857	0.940	24.220
W-Al 35	0.793	0.887	24.086
W-Rh 25	0.797	0.862	23.968
W-Rh 28	0.775	0.840	24.070
W-Rh 30	0.764	0.824	24.012
W-Rh 35	0.737	0.813	23.957
W-Ag 25	0.788	0.862	24.032
W-Ag 28	0.756	0.829	23.991
W-Ag 30	0.742	0.817	23.965
W-Ag 35	0.717	0.795	23.929
Mo-Rh 28	0.861	0.931	23.959
Mo-Rh 30	0.841	0.913	23.905
Mo-Rh 35	0.809	0.883	23.871
Mo-Mo 25	**0.995**	**1.066**	24.268
Mo-Mo 28	**0.939**	**1.014**	24.090
Mo-Mo 30	**0.911**	**0.986**	24.039
Mo-Mo 35	**0.863**	**1.056**	23.956

Table A.2: Calibration factors for the Piranha 657.

Piranha 657					
Applied radiation quality	**Calibration in the software**				
	W-Al	**W-Rh**	**W-Ag**	**Mo-Rh**	**Mo-Mo**
W-Al 25	**0.972**	1.144	1.054	1.282	1.291
W-Al 28	**1.031**	1.225	1.080	1.280	1.249
W-Al 30	**1.100**	1.256	1.215	1.003	0.910
W-Al 35	**1.188**	1.245	1.070	0.935	0.848
W-Rh 25	0.934	**0.972**	0.894	1.092	1.102
W-Rh 28	0.849	**1.017**	0.910	1.119	1.106
W-Rh 30	0.879	**1.055**	0.933	1.132	1.108
W-Rh 35	0.948	**1.086**	0.977	0.875	0.793
W-Ag 25	0.882	1.057	**0.941**	1.154	1.134
W-Ag 28	0.924	1.090	**0.961**	1.132	1.108
W-Ag 30	0.939	1.088	**0.975**	0.879	0.797
W-Ag 35	0.981	1.088	**1.013**	0.852	0.772
Mo-Rh 28	0.839	1.002	0.925	**1.108**	1.124
Mo-Rh 30	0.845	1.000	0.923	**1.115**	1.128
Mo-Rh 35	0.875	1.039	0.939	**1.145**	0.862
Mo-Mo 25	0.811	1.270	0.941	0.898	**0.980**
Mo-Mo 28	0.822	1.031	0.930	0.926	**1.063**
Mo-Mo 30	0.838	1.024	0.940	1.029	**1.112**
Mo-Mo 35	0.890	1.047	0.964	1.173	**1.181**

Table A.3: Calibration factors for the Black Piranha.

Black Piranha					
Applied radiation quality	**Calibration in the software**				
	W-Al	**W-Rh**	**W-Ag**	**Mo-Rh**	**Mo-Mo**
W-Al 25	**1.009**	1.189	1.178	1.185	1.107
W-Al 28	**1.011**	1.207	1.180	1.167	1.061
W-Al 30	**1.005**	1.185	1.176	1.127	1.025
W-Al 35	**1.000**	1.156	1.159	1.057	0.961
W-Rh 25	0.850	**1.005**	0.992	0.997	0.931
W-Rh 28	0.849	**1.021**	0.988	0.993	0.919
W-Rh 30	0.848	**1.019**	0.986	0.988	0.908
W-Rh 35	0.862	**1.019**	1.009	0.974	0.885
W-Ag 25	0.863	1.038	**1.003**	1.008	0.933
W-Ag 28	0.865	1.031	**1.011**	0.996	0.903
W-Ag 30	0.863	1.022	**1.010**	0.979	0.891
W-Ag 35	0.862	1.008	**1.009**	0.947	0.861
Mo-Rh 28	0.894	1.048	1.047	**1.044**	0.986
Mo-Rh 30	0.886	1.040	1.037	**1.039**	0.975
Mo-Rh 35	0.883	1.060	1.028	**1.034**	0.959
Mo-Mo 25	0.951	1.123	1.100	1.004	**0.997**
Mo-Mo 28	0.930	1.098	1.084	1.015	**1.012**
Mo-Mo 30	0.924	1.086	1.081	1.046	**1.016**
Mo-Mo 35	0.923	1.091	1.078	1.083	**1.018**

Table A.4: Calibration factors for the Nomex.

Nomex					
Applied radiation quality	**Calibration in the software**				
	W-Al	**W-Rh**	**W-Ag**	**Mo-Rh**	**Mo-Mo**
W-Al 25	**1.099**	1.149	1.131	1.087	1.085
W-Al 28	**1.088**	1.133	1.115	1.121	1.146
W-Al 30	**1.085**	1.128	1.111	1.148	1.193
W-Al 35	**1.083**	1.119	1.102	1.216	1.313
W-Rh 25	0.981	**1.021**	1.005	1.016	1.041
W-Rh 28	0.978	**1.016**	1.000	1.033	1.072
W-Rh 30	0.978	**1.015**	1.000	1.046	1.094
W-Rh 35	0.979	**1.014**	0.999	1.079	1.150
W-Ag 25	0.988	1.028	**1.012**	1.038	1.073
W-Ag 28	0.990	1.026	**1.010**	1.081	1.145
W-Ag 30	0.991	1.026	**1.010**	1.101	1.180
W-Ag 35	0.995	1.026	**1.010**	1.144	1.255
Mo-Rh 28	1.011	1.056	1.040	**1.012**	1.018
Mo-Rh 30	1.001	1.044	1.028	**1.011**	1.021
Mo-Rh 35	0.985	1.026	1.010	**1.012**	1.033
Mo-Mo 25	1.092	1.146	1.128	1.040	**1.018**
Mo-Mo 28	1.060	1.110	1.094	1.028	**1.015**
Mo-Mo 30	1.045	1.093	1.077	1.024	**1.018**
Mo-Mo 35	1.021	1.066	1.050	1.022	**1.027**

Table A.5: Calibration factors for the Xi.

Xi					
Applied radiation quality	**Calibration in the software**				
	W-Al	**W-Rh**	**W-Ag**	**Mo-Rh**	**Mo-Mo**
W-Al 25	**1.023**	1.099	1.158	1.018	1.004
W-Al 28	**1.026**	1.095	1.154	1.019	1.007
W-Al 30	**1.028**	1.094	1.157	1.021	1.012
W-Al 35	**1.028**	1.092	1.157	1.025	1.020
W-Rh 25	0.985	**1.017**	1.018	0.989	0.989
W-Rh 28	0.989	**1.017**	1.007	0.994	0.998
W-Rh 30	0.987	**1.018**	1.005	0.995	0.998
W-Rh 35	0.988	**1.019**	0.985	0.997	1.002
W-Ag 25	0.994	1.025	**1.004**	0.999	1.000
W-Ag 28	0.995	1.027	**1.009**	1.002	1.008
W-Ag 30	0.995	1.027	**1.007**	1.004	1.010
W-Ag 35	0.995	1.031	**1.004**	1.008	1.017
Mo-Rh 28	0.997	1.039	1.045	**0.996**	0.992
Mo-Rh 30	0.994	1.034	1.025	**0.992**	0.993
Mo-Rh 35	0.990	1.024	0.978	**0.993**	0.992
Mo-Mo 25	1.014	1.087	1.148	1.010	**0.999**
Mo-Mo 28	1.008	1.067	1.083	1.006	**0.997**
Mo-Mo 30	1.005	1.059	1.047	1.003	**0.996**
Mo-Mo 35	0.996	1.044	0.984	0.995	**0.990**

Table A.6: Calibration factors for the Accu Gold.

Accu Gold				
Applied radiation quality	**Calibration in the software**			
	W-Rh	**W-Ag**	**Mo-Rh**	**Mo-Mo**
W-Al 25	0.986	1.001	0.989	–
W-Al 28	0.994	0.989	–	–
W-Al 30	1.004	0.988	–	–
W-Al 35	–	–	–	–
W-Rh 25	**0.994**	1.000	1.022	–
W-Rh 28	**0.992**	0.997	1.032	–
W-Rh 30	**0.992**	0.992	–	–
W-Rh 35	**0.990**	0.985	–	–
W-Ag 25	0.990	**0.991**	1.031	–
W-Ag 28	0.996	**0.992**	–	–
W-Ag 30	0.999	**0.991**	–	–
W-Ag 35	–	**0.991**	–	–
Mo-Rh 28	1.006	1.008	**1.010**	1.024
Mo-Rh 30	1.003	1.005	**1.009**	1.020
Mo-Rh 35	0.986	0.992	**1.011**	1.026
Mo-Mo 25	1.014	1.019	1.041	**1.008**
Mo-Mo 28	1.017	1.017	1.029	**1.006**
Mo-Mo 30	1.012	1.010	1.010	**1.005**
Mo-Mo 35	0.985	0.989	0.986	**1.000**

Table A.7: Calibration factors for the X2.

X2					
Applied radiation quality	**Calibration in the software**				
	W-Al	**W-Rh**	**W-Ag**	**Mo-Rh**	**Mo-Mo**
W-Al 25	**1.013**	1.014	1.014	1.013	1.013
W-Al 28	**1.023**	1.022	1.021	1.022	1.023
W-Al 30	**1.026**	1.024	1.024	1.024	1.024
W-Al 35	**1.024**	1.024	1.024	1.025	1.025
W-Rh 25	0.992	**0.991**	0.992	0.992	0.992
W-Rh 28	0.994	**0.995**	0.995	0.994	0.995
W-Rh 30	0.995	**0.997**	0.996	0.996	0.995
W-Rh 35	0.992	**0.991**	0.992	0.991	0.990
W-Ag 25	0.993	0.993	**0.992**	0.992	0.994
W-Ag 28	0.994	0.993	**0.994**	0.992	0.993
W-Ag 30	0.995	0.993	**0.994**	0.994	0.994
W-Ag 35	0.990	0.990	**0.990**	0.989	0.990
Mo-Rh 28	1.007	1.005	1.005	**1.008**	1.006
Mo-Rh 30	1.007	1.007	1.007	**1.006**	1.007
Mo-Rh 35	1.006	1.007	1.006	**1.006**	1.007
Mo-Mo 25	1.002	1.002	1.002	1.001	**1.001**
Mo-Mo 28	1.012	1.012	1.010	1.010	**1.009**
Mo-Mo 30	1.012	1.011	1.012	1.012	**1.013**
Mo-Mo 35	1.009	1.010	1.008	1.008	**1.009**

Table A.8: HVL ratio measured by Black Piranha.

Black Piranha					
Applied radiation quality	**Calibration in the software**				
	W-Al	**W-Rh**	**W-Ag**	**Mo-Rh**	**Mo-Mo**
W-Al 25	**0.985**	0.742	0.741	0.721	0.781
W-Al 28	**1.013**	0.682	0.729	0.720	0.797
W-Al 30	**1.013**	0.675	0.701	0.733	0.819
W-Al 35	**1.005**	0.733	0.689	–	–
W-Rh 25	1.412	**1.027**	1.031	1.006	1.103
W-Rh 28	1.435	**1.014**	1.035	1.020	1.126
W-Rh 30	1.447	**0.965**	1.039	1.032	1.144
W-Rh 35	1.414	**0.957**	0.964	1.037	1.164
W-Ag 25	1.387	0.982	**1.001**	0.985	1.087
W-Ag 28	1.431	0.953	**0.993**	1.034	1.154
W-Ag 30	1.447	0.977	**0.988**	1.059	1.188
W-Ag 35	1.450	1.028	**0.985**	–	–
Mo-Rh 28	1.241	0.937	0.936	**0.911**	0.987
Mo-Rh 30	1.278	0.953	0.951	**0.925**	1.006
Mo-Rh 35	1.325	0.955	0.963	**0.942**	1.035
Mo-Mo 25	1.044	0.750	0.791	0.850	**0.903**
Mo-Mo 28	1.089	0.829	0.849	0.856	**0.913**
Mo-Mo 30	1.122	0.859	1.122	0.856	**0.919**
Mo-Mo 35	1.179	0.876	0.875	0.948	**0.926**

Table A.9: HVL ratio measured by Nomex.

Nomex					
Applied radiation quality	**Calibration in the software**				
	W-Al	**W-Rh**	**W-Ag**	**Mo-Rh**	**Mo-Mo**
W-Al 25	**0.791**	0.665	0.723	0.723	0.782
W-Al 28	**0.730**	0.618	0.677	–	–
W-Al 30	**0.781**	0.638	0.656	–	–
W-Al 35	**0.741**	–	–	–	–
W-Rh 25	1.181	**0.987**	1.081	1.081	1.167
W-Rh 28	1.195	**0.945**	1.093	1.102	–
W-Rh 30	1.202	**0.941**	1.089	–	–
W-Rh 35	1.168	**0.937**	0.991	–	–
W-Ag 25	1.141	0.898	**1.041**	–	–
W-Ag 28	1.174	0.929	**1.008**	–	–
W-Ag 30	1.189	0.954	**1.009**	–	–
W-Ag 35	1.177	1.002	**1.000**	–	–
Mo-Rh 28	1.048	0.901	0.956	**0.968**	1.039
Mo-Rh 30	1.070	0.920	0.979	**0.981**	1.062
Mo-Rh 35	1.094	0.884	0.999	**1.004**	–
Mo-Mo 25	0.856	0.713	0.771	0.940	**0.949**
Mo-Mo 28	0.927	0.785	0.847	0.863	**0.948**
Mo-Mo 30	0.949	0.813	0.866	0.914	**0.952**
Mo-Mo 35	0.966	0.815	0.883	0.883	**0.956**

Table A.10: HVL ratio measured by Xi.

Xi					
Applied radiation quality	**Calibration in the software**				
	W-Al	**W-Rh**	**W-Ag**	**Mo-Rh**	**Mo-Mo**
W-Al 25	**0.958**	0.843	0.911	0.897	0.914
W-Al 28	**0.973**	0.812	0.908	0.869	0.871
W-Al 30	**0.959**	0.782	0.896	0.852	0.846
W-Al 35	**0.902**	0.733	0.866	0.820	0.812
W-Rh 25	0.961	**0.965**	0.994	0.987	0.975
W-Rh 28	0.959	**0.954**	0.986	0.964	0.951
W-Rh 30	0.970	**0.956**	0.991	0.966	0.953
W-Rh 35	1.019	**0.955**	1.007	0.953	0.945
W-Ag 25	0.970	0.957	**0.993**	0.958	0.947
W-Ag 28	0.974	0.940	**0.984**	0.950	0.939
W-Ag 30	0.970	0.930	**0.978**	0.947	0.938
W-Ag 35	0.982	0.921	**0.973**	0.939	0.937
Mo-Rh 28	0.954	0.949	0.978	**0.972**	0.966
Mo-Rh 30	0.984	0.961	0.994	**0.972**	0.965
Mo-Rh 35	1.073	0.999	1.044	**0.977**	0.966
Mo-Mo 25	0.902	0.878	0.899	0.941	**0.963**
Mo-Mo 28	0.955	0.919	0.945	0.952	**0.966**
Mo-Mo 30	1.008	0.945	0.979	0.957	**0.966**
Mo-Mo 35	1.148	0.992	1.054	0.963	**0.964**

Table A.11: HVL ratio measured by Accu Gold, AGMS -DM+.

Accu Gold					
Applied radiation quality	**Calibration in the software**				
	W-Al	**W-Rh**	**W-Ag**	**Mo-Rh**	**Mo-Mo**
W-Al 25	–	0.311	0.356	0.310	–
W-Al 28	–	0.356	0.360	–	–
W-Al 30	–	0.390	0.385	–	–
W-Al 35	–	–	–	–	–
W-Rh 25	–	**0.461**	0.465	0.487	–
W-Rh 28	–	**0.500**	0.496	0.528	–
W-Rh 30	–	**0.517**	0.511	–	–
W-Rh 35	–	**0.550**	0.538	–	–
W-Ag 25	–	0.478	**0.476**	0.509	–
W-Ag 28	–	0.541	**0.496**	0.496	–
W-Ag 30	–	0.572	**0.559**	0.559	–
W-Ag 35	–	–	–	–	–
Mo-Rh 28	–	0.395	0.397	**0.393**	0.408
Mo-Rh 30	–	0.407	0.412	**0.415**	0.432
Mo-Rh 35	–	0.431	0.431	**0.452**	0.471
Mo-Mo 25	–	0.299	0.301	0.306	**0.293**
Mo-Mo 28	–	0.336	0.335	0.329	**0.325**
Mo-Mo 30	–	0.352	0.350	0.340	**0.343**
Mo-Mo 35	–	0.365	0.370	0.369	**0.381**

Table A.12: HVL ratio measured by X2.

X2					
Applied radiation quality	**Calibration in the software**				
	W-Al	**W-Rh**	**W-Ag**	**Mo-Rh**	**Mo-Mo**
W-Al 25	**1.039**	1.035	1.034	1.038	1.038
W-Al 28	**1.034**	1.035	1.037	1.034	1.033
W-Al 30	**1.023**	1.023	1.024	1.024	1.023
W-Al 35	**0.999**	0.999	0.998	0.997	0.998
W-Rh 25	1.005	**1.005**	1.004	1.004	1.004
W-Rh 28	0.986	**0.987**	0.985	0.984	0.985
W-Rh 30	0.989	**0.986**	0.986	0.988	0.990
W-Rh 35	0.993	**0.995**	0.993	0.996	0.997
W-Ag 25	1.001	1.001	**1.001**	1.002	0.998
W-Ag 28	0.993	0.993	**0.991**	0.993	0.992
W-Ag 30	0.989	0.992	**0.988**	0.989	0.989
W-Ag 35	0.989	0.991	**0.990**	0.990	0.989
Mo-Rh 28	0.991	0.992	0.992	**0.990**	0.992
Mo-Rh 30	0.988	0.987	0.987	**0.990**	0.988
Mo-Rh 35	0.993	0.991	0.994	**0.993**	0.993
Mo-Mo 25	0.971	0.969	0.972	0.971	**0.972**
Mo-Mo 28	0.978	0.978	0.982	0.979	**0.980**
Mo-Mo 30	0.988	0.989	0.988	0.985	**0.988**
Mo-Mo 35	1.006	1.005	1.007	1.007	**1.006**

Table A.13: *kVp* ratio measured by Piranha 657.

Piranha 657					
Applied radiation quality	**Calibration in the software**				
	W-Al	**W-Rh**	**W-Ag**	**Mo-Rh**	**Mo-Mo**
W-Al 25	**0.970**	1.021	1.034	0.729	0.676
W-Al 28	**0.965**	0.854	1.005	0.646	0.611
W-Al 30	**0.967**	0.826	0.942	–	–
W-Al 35	**0.969**	0.836	–	–	–
W-Rh 25	–	**0.998**	1.020	0.702	0.660
W-Rh 28	1.030	**1.006**	1.091	0.713	0.690
W-Rh 30	1.073	**0.995**	1.127	0.724	0.702
W-Rh 35	1.140	**0.988**	1.149		
W-Ag 25	0.915	0.885	**0.968**	0.631	0.611
W-Ag 28	0.953	0.834	**0.992**	0.644	0.594
W-Ag 30	0.991	0.854	**1.001**	–	–
W-Ag 35	1.075	0.911	**0.990**	–	–
Mo-Rh 28	1.131	1.200	1.200	**0.912**	0.817
Mo-Rh 30	1.186	1.257	1.264	**0.929**	0.841
Mo-Rh 35	1.308	1.319	1.393	**0.926**	0.888
Mo-Mo 25	1.136	–	1.194	1.124	**0.978**
Mo-Mo 28	1.213	1.272	1.271	1.185	**0.958**
Mo-Mo 30	1.257	1.328	1.324	1.139	**0.947**
Mo-Mo 35	1.354	1.425	1.445	1.012	**0.943**

Table A.14: *kVp* ratio measured by Black Piranha.

Black Piranha					
Applied radiation quality	**Calibration in the software**				
	W-Al	**W-Rh**	**W-Ag**	**Mo-Rh**	**Mo-Mo**
W-Al 25	**0.986**	1.014	1.030	0.719	0.679
W-Al 28	**0.986**	0.839	1.003	0.620	0.609
W-Al 30	**0.988**	0.819	0.922	–	–
W-Al 35	**0.992**	0.824	0.860	–	–
W-Rh 25	0.977	**0.992**	1.021	0.700	0.666
W-Rh 28	1.052	**0.975**	1.105	0.712	0.691
W-Rh 30	1.098	**0.972**	1.150	0.720	0.703
W-Rh 35	1.170	**0.971**	1.112	–	–
W-Ag 25	0.936	0.861	**0.983**	0.630	0.613
W-Ag 28	0.975	0.824	**0.980**	0.607	0.596
W-Ag 30	1.014	0.845	**0.979**	–	0.606
W-Ag 35	1.096	0.905	**0.965**	–	–
Mo-Rh 28	1.144	1.200	1.189	**0.908**	0.818
Mo-Rh 30	1.202	1.251	1.252	**0.907**	0.840
Mo-Rh 35	1.327	1.258	1.394	**0.909**	0.880
Mo-Mo 25	1.141	1.186	1.181	1.127	**0.975**
Mo-Mo 28	1.222	1.274	1.267	1.158	**0.961**
Mo-Mo 30	1.270	1.330	1.317	1.126	**0.951**
Mo-Mo 35	1.373	1.401	1.435	0.990	**0.939**

Table A.15: *kVp* ratio measured by Nomex.

Nomex					
Applied radiation quality	**Calibration in the software**				
	W-Al	**W-Rh**	**W-Ag**	**Mo-Rh**	**Mo-Mo**
W-Al 25	1.000	1.008	1.020	0.718	0.665
W-Al 28	1.018	0.820	0.986	–	–
W-Al 30	1.010	0.794	0.901	–	–
W-Al 35	1.017	–	–	–	–
W-Rh 25	0.996	**1.000**	1.016	0.710	0.660
W-Rh 28	1.077	**0.989**	1.102	0.722	–
W-Rh 30	1.128	**0.974**	1.149	–	–
W-Rh 35	1.215	**0.965**	1.129	–	
W-Ag 25	0.958	0.859	**0.977**	–	–
W-Ag 28	1.000	0.809	**0.969**	–	–
W-Ag 30	1.042	0.826	**0.968**	–	–
W-Ag 35	1.133	0.888	**0.964**	–	–
Mo-Rh 28	1.167	1.202	1.186	**0.924**	0.824
Mo-Rh 30	1.230	1.261	1.250	**0.927**	0.845
Mo-Rh 35	1.367	1.306	1.394	**0.936**	–
Mo-Mo 25	1.131	1.136	1.136	1.106	**0.965**
Mo-Mo 28	1.233	1.256	1.250	1.162	**0.956**
Mo-Mo 30	1.288	1.322	1.304	1.119	**0.949**
Mo-Mo 35	1.406	1.417	1.434	1.012	**0.936**

Table A.16: *kVp* ratio measured by Xi.

Xi					
Applied radiation quality	**Calibration in the software**				
	W-Al	**W-Rh**	**W-Ag**	**Mo-Rh**	**Mo-Mo**
W-Al 25	**0.992**	0.930	–	–	0.711
W-Al 28	**0.989**	0.831	–	–	–
W-Al 30	**0.985**	0.821	–	–	–
W-Al 35	**0.973**	–	–	0.951	1.432
W-Rh 25	1.011	**1.003**	–	–	–
W-Rh 28	1.096	**0.982**	–	–	–
W-Rh 30	1.144	**0.977**	–	–	–
W-Rh 35	1.222	**0.976**	–	1.104	–
W-Ag 25	0.967	0.844	–	–	–
W-Ag 28	1.017	0.826	–	0.836	–
W-Ag 30	1.061	0.846	–	0.957	–
W-Ag 35	1.155	0.895	–	1.038	–
Mo-Rh 28	1.167	1.188	–	**0.949**[11]	0.762
Mo-Rh 30	1.225	1.232	–	**0.951**[11]	0.739
Mo-Rh 35	1.352	1.180	–	**0.953**[11]	–
Mo-Mo 25	1.152	1.154	–	–	**0.974**
Mo-Mo 28	1.229	1.241	–	–	**0.960**
Mo-Mo 30	1.272	1.296	–	–	**0.949**
Mo-Mo 35	1.371	1.208	–	–	**0.934**

Table A.17: *kVp* ratio measured by Accu Gold, AGMS- DM+.

Accu Gold					
Applied radiation quality	**Calibration in the software**				
	W-Al	**W-Rh**	**W-Ag**	**Mo-Rh**	**Mo-Mo**
W-Al 25	–	0.926	0.992	0.744	–
W-Al 28	–	0.848	0.924	–	–
W-Al 30	–	0.820	0.882	–	–
W-Al 35	–	–	–	–	–
W-Rh 25	–	**0.964**	1.033	0.677	–
W-Rh 28	–	**0.972**	1.102	0.654	–
W-Rh 30	–	**0.974**	1.172	–	–
W-Rh 35	–	**0.972**	1.144	–	–
W-Ag 25	–	0.839	**0.984**	0.572	–
W-Ag 28	–	0.804	**1.102**	–	–
W-Ag 30	–	0.815	**0.960**	–	–
W-Ag 35	–	–	**0.964**	–	–
Mo-Rh 28	–	1.186	1.191	**0.924**	0.808
Mo-Rh 30	–	1.230	1.261	**0.935**	0.815
Mo-Rh 35	–	1.287	1.411	**0.938**	0.825
Mo-Mo 25	–	1.147	1.161	1.116	**0.996**
Mo-Mo 28	–	1.256	1.254	1.167	**0.996**
Mo-Mo 30	–	1.322	1.310	1.136	**0.993**
Mo-Mo 35	–	1.373	1.440	1.080	**0.986**

[11] Measured with additional 2 *mm* Al

Table A.18: *kVp* ratio measured by X2.

X2					
Applied radiation quality	**Calibration in the software**				
	W-Al	**W-Rh**	**W-Ag**	**Mo-Rh**	**Mo-Mo**
W-Al 25	1.015	1.000	0.976	–	1.425
W-Al 28	1.021	1.257	1.056	–	–
W-Al 30	1.024	1.263	1.232	1.079	–
W-Al 35	1.031	–	–	1.113	–
W-Rh 25	0.996	**1.008**	0.976	–	–
W-Rh 28	0.914	**1.021**	0.896	–	–
W-Rh 30	0.870	**1.027**	0.858	–	–
W-Rh 35	0.797	**1.040**	0.883	0.912	–
W-Ag 25	1.036	1.181	**1.024**	–	–
W-Ag 28	0.982	1.264	**1.013**	–	–
W-Ag 30	0.937	1.260	**1.023**	1.059	–
W-Ag 35	0.849	–	**1.029**	0.987	–
Mo-Rh 28	0.854	0.827	0.836	–	1.304
Mo-Rh 30	0.807	0.790	0.790	–	1.304
Mo-Rh 35	0.711	0.784	0.709	–	–
Mo-Mo 25	0.868	0.816	0.836	–	**1.028**
Mo-Mo 28	0.804	0.761	0.779	–	**1.039**
Mo-Mo 30	0.767	0.730	0.747	–	**1.047**
Mo-Mo 35	0.691	0.680	0.680	–	**1.063**

Acknowledgments

The measurements for this thesis were carried out during 2017 at the IAEA Dosimetry Laboratory in Seibersdorf, Austria. I would like to express my great appreciation to Paula Toroi, PhD, SSDL officer at the IAEA and Joanna Izewska, PhD, laboratory head of the IAEA Dosimetry Laboratory, for the opportunity to work in this project. From the Zentrum für Medizinische Physik und Biomedizinische Technik I wish to express my gratitude to Univ. Doz. Dr.techn. Peter Homolka.

I would like to offer my special thanks to my supervisors, Paula Toroi, PhD, Dr.techn. Peter Homolka, and Istvan Csete, PhD, for the help with this thesis and to introduce me to the field of medical physics and dosimetry. I am particularly grateful for the assistance and advice given by Istvan Csete, PhD and Ladislav Czap, MSc, for introducing and guiding me in the laboratory work at the IAEA DOL.

I would like to thank following companies and departments for their cooperation RTI, PTW, STUK, PTPA (MA 39) especially Josef Fuchs, for lending me dosimeters for this study free of charge. Thanks for the uncomplicated handling of the renting procedure and for being ready to answer all upcoming questions related to the instruments.

I am also grateful to all colleagues at IAEA for their interest in my work and make me feel as a full team member. Especially I want to thank Istvan, for taking care of my health conditions with lending me his bike and to Mirja and Luka for many interesting and informative discussions. I would like to express my very great appreciation to my beloved partner and best friend Harry for providing me with unfailing support and continuous encouragement throughout my years of study.

Bibliography

[1] INTERNATIONAL ELECTROTECHNICAL COMMISSION, "NORME INTERNATIONALE CEI/IEC 61267: Medical diagnostic X-ray equipment- Radiation condition for use in the determination of characteristics," 2005.

[2] INTERNATIONAL ELECTROTECHNICAL COMMISSION, "IEC 61674: Medical electrical equipment- Dosimeters with ionization chambers and/or semiconductor detectors as used in X-ray diagnostic imaging," 2009.

[3] WORLD HEALTH ORGANIZATION, "Breast cancer: prevention and control." [Online]. Available: http://www.who.int/cancer/detection/breastcancer/en/. [Accessed: 16-Jun-2017].

[4] E. K. J. Pauwels, N. Foray, and M. H. Bourguignon, "Breast Cancer Induced by X-Ray Mammography Screening? A Review Based on Recent Understanding of Low-Dose Radiobiology," *Med. Princ. Pract.*, vol. 25, no. 2, pp. 101–109, 2016.

[5] D. R. Dance, "Monte Carlo calculation of conversion factors for the estimation of mean glandular breast dose," *Phys. Med. Biol.*, vol. 35, no. 9, pp. 1211–1219, 1990.

[6] D. R. Dance, C. L. Skinner, K. C. Young, J. R. Beckett, and C. J. Kotre, "Additional factors for the estimation of mean glandular breast dose using the UK mammography dosimetry protocol.," *Phys. Med. Biol.*, vol. 45, no. 11, pp. 3225–3240, 2000.

[7] R. E. Dance, D R; Young, K C; van Engen, "Further factors for the estimation of mean glandular dose using the United Kingdom, European and IAEA breast dosimetry protocols," *Phys. Med. Biol.*, vol. 54, pp. 4361–4372, 2009.

[8] INTERNATIONAL ATOMIC ENERGY AGENCY, *Diagnostic Radiology Physics- A Handbook for Teachers and Students*. Vienna, 2014.

[9] J. T. Bushberg, A. Seibert, E. Leidholdt, and J. Boone, *The essential physics of medical imaging: Third Edition*. Wolters Kluwer| Lippincott Williams & Wilkins, 2002.

[10] BUREAU INTERNATIONAL DES POIDS ET MESURES, *International vocabulary of metrology — Basic and general concepts and associated terms (VIM)*. 2008.

[11] INTERNATIONAL ATOMIC ENERGY AGENCY, *SSDL Network Charter*, Second Edi. Vienna, 2017.

[12] INTERNATIONAL ATOMIC ENERGY AGENCY, *Dosimetry in Diagnostic Radiology: an Internacional Code of Practice- Technical Report Series No 457*. 2014.

[13] INTERNATIONAL ATOMIC ENERGY AGENCY, *IAEA HUMAN HEALTH SERIES No. 17- Quality Assurance Programme for Digital Mammography*. Vienna, 2011.

[14] "GE, Senographe Essential." [Online]. Available: http://www.medwow.com/med/digital-mammography-unit/ge-healthcare/senographe-essential/34092.model.spec. [Accessed: 13-Oct-2017].

[15] "Hologic." [Online]. Available: http://www.hologic.com/sites/default/files/DS-05534_rev_SeleniaDimensions13Jan2016.pdf. [Accessed: 04-Aug-2017].

[16] "Siemens Healthineers." [Online]. Available: https://www.healthcare.siemens.com/mammography/digital-mammography/mammomat-inspiration-prime/technical-specifications. [Accessed: 04-Aug-2017].

[17] "NCCPM." [Online]. Available: http://medphys.royalsurrey.nhs.uk/nccpm/?s=technicalevaluations. [Accessed: 13-Oct-2017].

[18] "Philips MicroDose." [Online]. Available: http://dcpgc.weebly.com/uploads/4/6/3/0/46300783/i50_technical_specifications.pdf. [Accessed: 13-Oct-2017].

[19] "Sectra MicroDose Mammography." [Online]. Available: http://dcpgc.weebly.com/uploads/4/6/3/0/46300783/l30_technical_specifications_.pdf. [Accessed: 13-Oct-2017].

[20] BUREAU INTERNATIONAL DES POIDS ET MESURES, "Measuring conditions and uncertainties for the comparison and calibration of National Dosimeteric Standards at the BIPM." 2011.

[21] PHYSIKALISCH-TECHNISCHE BUNDESANSTALT, "Calibration of secundary standards-complete list of radiation qualities available for calibrations," 2015.

[22] P. H. H. Libby F. Brateman, "Solid-state dosimeters: A new approach for mammography measurements," *Med. Phys.*, vol. 42, no. 2, pp. 542–557, 2015.

[23] T. K. Michiharu Sekimoto, Yoh Katoh, "Calibration coefficients of dosimeters used in mammography for various target/filter combinations," *J. Appl. Clin. Med. Phys.*, vol. 16, no. 6, pp. 401–410, 2015.

[24] INTERNATIONAL ATOMIC ENERGY AGENCY, "Appendix 3C DOLP.013: Appendix to IAEA calibration certificate diagnostic radiology ionization chamber calibration procedures at the IAEA Dosimetry Laboratory," 2011.

[25] "Specifications Radcal 10X5-6M." [Online]. Available: http://perlamar.ie/wp-content/uploads/pdf/radcal/Ion_Chambers_Misc_Meters/Radcal_10x5_Series_Ion_Chambers.pdf. [Accessed: 06-Feb-2017].

[26] RTI, *Piranha_and_QABrowser_Reference Manual - English - Version 4.3A*. 2012.

[27] RTI, "Barracuda & QA BrowserReference Manual - English - Version 4.3A," 2012.

[28] Unfors Instuments, *Manual for Mult-O-Meter*. 1997.

[29] RTI, "Piranha Reference Manual - English - Version 5.5G," 2016.

[30] UNFORS RaySafe, "RaySafe Xi, User Manual," vol. 5000071–L, 2014.

[31] PTW, *User Manual Nomex Multimeter T11049 and Nomex Software S030008*. 2007.

[32] RADCAL, "ACCU-GOLD User Guide," vol. 4094118 Re, 2010.

[33] UNFORS RaySafe, "RaySafe X2- Benutzerhandbuch," vol. 5001086–4, 2014.

[34] RaySafe, *RaySafe X2 Specifications*. 2016.

[35] PTW, “Instruction Manual: inozation Chambers Type 77335 and Type 77334 with Check Sourch Type 894,” vol. D391.131.0.

[36] INTERNATIONAL ATOMIC ENERGY AGENCY, *DOLP.013 Calibration Service for Reference Dosimeters for Diagnostic Radiology- Quality Management System Procedures*. 2016.

[37] I. and O. Joint Committee for Guidedes in Metrology (BIPM, IEC, IFCC, ISO, IUPAC, *Evaluation of measurement data — Guide to the expression of uncertainty in measurement*, vol. JCGM 100:2. 2008.

[38] INTERNATIONAL ATOMIC ENERGY AGENCY, “Measurement Uncertainty: A Practical Guide for Secondary Standards Dosimetry Laboratories,” no. IAEA-TECDOC-1585, 2008.

List of tables

List of figures